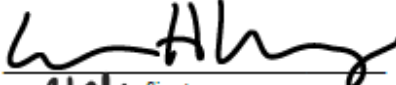



Natalie Packard

Triple oxygen and clumped isotope records from Bear Lake (Utah/Idaho) since the last glacial maximum and implications for paleohydrology and paleoclimate

submitted in partial fulfillment of the requirements for the degree of
Master of Science in Earth and Environmental Sciences
Department of Earth and Environmental Sciences
The University of Michigan

 Signature	Accepted by: Benjamin H. Passey Name	21 June 2022 Date
 Signature	Dr. Nathan Sheldon Name	18 July 2022 Date
Marin Clark Department Chair Signature	Marin K. Clark Name	17 Aug 2022 Date

I hereby grant the University of Michigan, its heirs and assigns, the non-exclusive right to reproduce and distribute single copies of my thesis, in whole or in part, in any format. I represent and warrant to the University of Michigan that the thesis is an original work, does not infringe or violate any rights of others, and that I make these grants as the sole owner of the rights to my thesis. I understand that I will not receive royalties for any reproduction of this thesis.

- Permission granted.
- Permission granted to copy after: _____
- Permission declined.


Author Signature



Triple oxygen and clumped isotope records from Bear Lake (Utah/Idaho) since the last glacial maximum and implications for paleohydrology and paleoclimate

Natalie Packard

Department of Earth and Environmental Sciences, University of Michigan, Ann Arbor, Michigan, USA

A Master's Thesis written as a manuscript for submission to Quaternary Research, to be co-authored with Benjamin Passey. This thesis includes an extended abstract that will not be part of the submitted manuscript.

ABSTRACT

We applied triple oxygen isotopes, clumped isotopes, and stepped-temperature acid digestions to lacustrine sediments from the past 25 ka from Bear Lake (Utah / Idaho) to better understand the hydrological and climatic evolution of the lake basin. Elevated clumped isotope temperatures ($> 30\text{ }^{\circ}\text{C}$) from the late glacial portion of the core (25 to 16 ka) indicate that detrital carbonate influences the isotopic measurements from this part of the record. Use of low temperature ($25\text{ }^{\circ}\text{C}$) acid digestion minimizes the influence of detrital carbonate. We develop an interpretive framework that allows for environmental inferences despite the detrital contamination. Lake water $\delta^{18}\text{O}$ shifted by at least $+4\text{‰}$ from the late glacial to the Holocene, while lake water $\Delta^{17}\text{O}$ decreased by at least 0.02‰ , indicating that the change in $\delta^{18}\text{O}$ was largely driven by increased evaporation. Evaporation from the late glacial lake accounted for $\sim >40\%$ of the water efflux from the lake, while the Holocene Lake was generally endorheic (100% evaporative efflux). We do not observe marked change in the $\delta^{18}\text{O}$ of pristine (unevaporated) catchment precipitation from late glacial ($-15.7 \pm 1.8\text{‰}$) to Holocene time ($-15.0 \pm 1.1\text{‰}$), although this is a minimum estimate of change.

EXTENDED ABSTRACT

Lacustrine carbonate stable isotope ($\delta^{13}\text{C}$, $\delta^{18}\text{O}$) records are an important source of paleoclimate information, yet their interpretation is hindered by the multiple influences, including evaporation and presence of detrital carbonate. In lakes where the evaporative efflux represents a large proportion of total water efflux, $\delta^{18}\text{O}$ values can be increased by many per mil over catchment precipitation $\delta^{18}\text{O}$. It has recently been shown that high precision measurements of triple oxygen isotope anomalies ($\Delta^{17}\text{O}$) in modern lacustrine carbonates allow for these evaporative effects to be identified. Furthermore, clumped isotopes may provide information about detrital carbonate contamination because ancient marine

carbonates commonly have elevated clumped isotope temperatures (ca. > 50 °C) due to burial diagenesis. The late-glacial to present sedimentary record from Bear Lake (Utah / Idaho) presents an excellent opportunity to apply and evaluate these new isotopic systems. Detrital carbonate is known to be present in these sediments and can constitute a significant fraction of carbonate during glacial stages. The existing $\delta^{13}\text{C}$ and $\delta^{18}\text{O}$ record from Bear Lake shows dramatic positive shifts from the Last Glacial Maximum (LGM) into the Holocene, which along with mineralogical data have been interpreted as a shift towards more arid, evaporative conditions. If true, we should observe a corresponding shift in the triple oxygen isotope record, from high $\Delta^{17}\text{O}$ values during the late glacial period to lower values during the Holocene.

We analyzed triple oxygen isotopes and clumped isotopes of core sediment from 0.02 to 15 meters below lake floor (mblf) spanning approximately 0.2 ka to 24.6 ka. Clumped isotope temperatures from the younger (~10.1 ka to present) carbonate-rich (~75% carbonate, as aragonite) portion of the core yield realistic paleotemperatures of $17 \pm 6^\circ\text{C}$ (mean $\pm 1\sigma$). However, in the older (~ 24.6 ka to 11.6 ka) carbonate-poor (<20% carbonate, primarily as calcite and dolomite) portion of the record, clumped isotope temperatures were unrealistically high ($40 \pm 12^\circ\text{C}$). The apparent clumped isotope temperatures of Paleozoic and Mesozoic dolomitic strata in the region averaged $85 \pm 16^\circ\text{C}$. Thus, the high clumped isotope temperatures in the older part of the core are consistent with contamination by detrital dolomite.

We further investigated the influence of detrital dolomite contamination using stepped-temperature acid digestion reactions of the lake carbonate, where calcite/aragonite should be preferentially reacted at a lower temperature (25°C), and the remaining fraction (presumably enriched in dolomite) then reacted by increasing the temperature to 50°C following extraction of the gas released at 25°C. As part of this investigation, we present novel data on the temperature dependence of triple oxygen isotope fractionation during acid digestion of carbonates. These stepped-temperature results are consistent with detrital carbonate contamination, and the effects are consistent with all four isotope measurements evaluated ($\delta^{13}\text{C}$, $\delta^{18}\text{O}$, $\Delta^{17}\text{O}$, Δ_{47}). Owing to this contamination, which is not completely

avoided even with using the lowest temperature (25°C) acid digestions, we interpret the late glacial triple oxygen isotope data as placing *upper limits* on $\delta^{18}\text{O}$ and *lower limits* on $\Delta^{17}\text{O}$ values of authigenic carbonates.

Based on this interpretive framework, and with conservative assumptions about temperatures of authigenic carbonate formation in the late glacial portion of the record for which clumped isotope temperatures are unreliable, we estimate that $\delta^{18}\text{O}$ values of lake waters increased by at least 4‰ from the late glacial to the Holocene (from $-8.6 \pm 0.7\text{‰}$ to $-4.6 \pm 1.5\text{‰}$), and $\Delta^{17}\text{O}$ values of the waters decreased by at least 0.02‰ (from $-0.002 \pm 0.011\text{‰}$ to $-0.022 \pm 0.008\text{‰}$). Importantly, the $\Delta^{17}\text{O}$ values show that (1) nearly all of the shift in $\delta^{18}\text{O}$ was due to increased evaporation from the lake following late glacial times, and (2) the glacial lake, while less evaporated than the Holocene lake, was nonetheless strongly modified by evaporation. Using $\Delta^{17}\text{O}$ to ‘strip-off’ the effects of evaporation, we calculate the minimum change in $\delta^{18}\text{O}$ of catchment precipitation between the late glacial and Holocene (from $-15.7 \pm 1.8\text{‰}$ to $-15.0 \pm 1.1\text{‰}$). This approximate degree of change in $\delta^{18}\text{O}$ of precipitation following the late glacial has also been simulated by isotope-enabled Earth System Models and suggested by other oxygen isotope records from the western U.S. (i.e., Devil’s Hole). This study demonstrates how the addition of $\Delta^{17}\text{O}$ and Δ_{47} data can significantly improve our understanding of stable isotope records from lacustrine sediments, and the hydrological and paleoclimatic significance thereof.

INTRODUCTION

Anthropogenic impacts to western North American climate and surface hydrology are projected to decrease water availability over the next century as both carbon dioxide levels and temperature increase (Barnett et al., 2008; Broecker, 2010; Freidrich et al., 2017). Studying past lake systems during intervals where large climate shifts have occurred provides perspective on the sensitivity of lake systems to climate change. Oxygen isotopes ($\delta^{18}\text{O}$) of lacustrine carbonate sediments have been commonly used

as a tool for reconstructing past climate and hydrology (Dinçer, 1968; Leng and Marshall, 2004; Gibson et al., 2015), but the interpretation of this data is complicated by the many factors that influence lacustrine carbonate $\delta^{18}\text{O}$. These factors include the $\delta^{18}\text{O}$ of lake catchment precipitation (which relates to regional climate), the relative evaporation efflux of water from the lake (expressed as X_E , where $X_E = \text{evaporative water efflux} / \text{total water efflux}$), seasonal timing and temperature during carbonate mineralization, and contamination of the authigenic signal by detrital carbonate.

In this study, we explore the use of triple oxygen and clumped isotopes in lake carbonates to help constrain some of these factors. Both of these measurements are relatively new in terms of analytical capability (mid-late 2010's for triple oxygen isotopes and mid-2000's for clumped isotopes), and we believe that this is the first study to combine these measurements for the study of ancient lacustrine carbonate sediments. Our study system is the late-glacial (25 ka) to present record from core GLAD800-BL00-1E retrieved from Bear Lake (Utah / Idaho) in September 2000 and archived at the LacCore facility (now Continental Scientific Drilling Facility, Minneapolis, Minnesota) (Figure 1). Previous work has documented dramatic increases in both $\delta^{13}\text{C}$ and $\delta^{18}\text{O}$ of lake carbonate during the transition from cold late glacial climates into warmer Holocene climates (Bright et al., 2006; Kaufman et al., 2009). This has been interpreted to reflect the retraction of the lake into a topographically closed basin in response to warmer and drier conditions. However, other factors can also drive changes in isotopic compositions, including changes in the $\delta^{18}\text{O}$ of precipitation falling in the catchment, and changes in the proportion of authigenic versus detrital carbonate. As described below, triple oxygen isotopes and clumped isotopes are uniquely suited to answer such questions. Ultimately, the goals of this study are two-fold: to learn more about the application and systematics of triple and clumped isotopes in lacustrine carbonates, and to better understand the paleohydrology of Bear Lake in response to the late glacial to Holocene climatic transition in the western United States.

In this paper, we first provide background on triple oxygen isotopes, clumped isotope thermometry, and our study system, Bear Lake. We then describe the analytical methods used in this study, and initial results. We discuss how stepped acid digestion experiments confirm the influence of detrital carbonate, and how despite this contamination we can still place useful directional constraints on isotopic compositions and magnitudes of isotopic change. We discuss implications for Bear Lake paleohydrology and compare our isotopic records with other records from the western United States and predictions from an isotope enabled Earth System Model. We conclude with a summary of the findings of this study, and possible areas for future study.

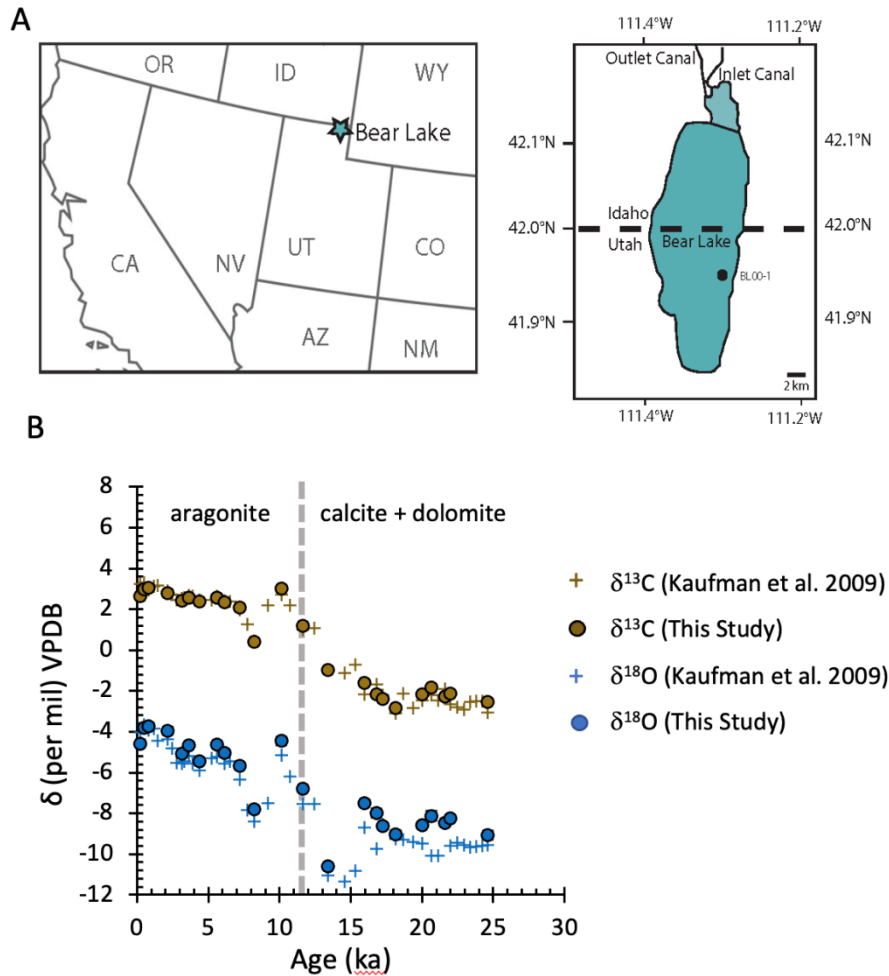


Figure 1. Geographical location of the study area, and existing isotopic record from core BL00-1E. A) Location map of Bear Lake, Utah/Idaho showing core site BL00-1E (black circle). The inlet and outlet canals shown on the north end of the lake are human-made canals that connect the lake with Bear River. B) Existing $\delta^{13}\text{C}$ and $\delta^{18}\text{O}$ records from bulk lacustrine carbonate (brown and blue + signs, respectively, Kaufman et al., 2009) compared with $\delta^{13}\text{C}$ and $\delta^{18}\text{O}$ values produced during clumped isotope analyses of bulk lacustrine carbonate for this study (brown and blue circles, respectively). The shift from lower $\delta^{13}\text{C}$ and $\delta^{18}\text{O}$ values during the late glacial period to higher values in the Holocene, which has been interpreted as an increase in evaporative efflux from the lake. The isotopic shift is accompanied by a shift in dominant carbonate mineralogy, from calcite and dolomite in the late glacial to aragonite in the Holocene. Also note a consistent positive offset in $\delta^{18}\text{O}$ values of our analyses compared to those made by Kaufman et al., (2009), which likely reflects a greater contribution of detrital dolomite in our measurements due to the higher acid digestion temperature in our lab (90 °C, versus 70 °C used by Kaufman et al., (2009)).

BACKGROUND

Triple Oxygen isotopes

Before discussing triple oxygen isotopes, it is useful to recall the ‘traditional’ oxygen isotope ($^{18}\text{O}/^{16}\text{O}$) and hydrogen isotope ($^2\text{H}/^1\text{H}$) system, which has long been used in the study of climate and paleoclimate (Urey, 1948; Craig, 1961; Dansgaard 1964; Dincer, 1968; Gat, 1996). A linear correlation exists between hydrogen and oxygen isotope ratios in global precipitation (Figure 2A), and is referred to as the global meteoric water line (GMWL), which follows the relationship:

$$\delta\text{D} = 8 * \delta^{18}\text{O} + 10$$

Equation 1

where $\delta = (R_{\text{sample}} / R_{\text{standard}} - 1) \times 1000$, and R is the abundance ratio of the isotopically-substituted isotopologue to the common isotopologue (e.g., $^{18/16}R = ^{12}\text{C}^{18}\text{O}^{16}\text{O} / ^{12}\text{C}^{16}\text{O}_2$). Here, the slope of 8 reflects the ratio of the $^2\text{H}/^1\text{H}$ and $^{18}\text{O}/^{16}\text{O}$ equilibrium fractionation factors between liquid water and water vapor (i.e., $^{2/1}\alpha_{\text{l-v}} / ^{18/16}\alpha_{\text{l-v}} \approx 8$) that dominates the physics of Rayleigh distillation of atmospheric vapor masses. Evaporation, on the other hand, involves kinetic fractionations where the ratio of the $^2\text{H}/^1\text{H}$ and $^{18}\text{O}/^{16}\text{O}$ fractionation factors is variable but smaller than 8 (Figure 2A). Therefore, waters subjected to significant evaporative loss plot ‘below’ the meteoric water line and evolve along slopes lower than 8. Deviation

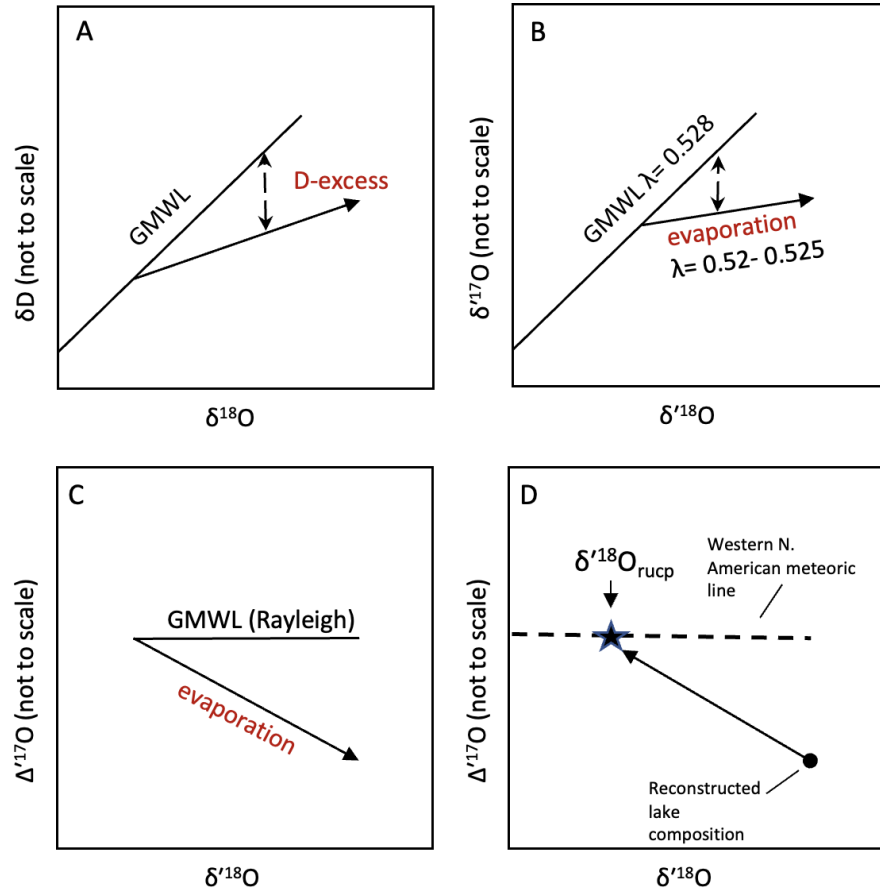


Figure 2. Schematic diagram comparing isotope hydrology in $\delta D - \delta^{18}O$ space and isotope hydrology in triple oxygen isotope space. A). ‘Traditional’ $\delta D - \delta^{18}O$ hydrology, showing the global meteoric water line (GMWL) along which most precipitation plots, and an evaporation trajectory (arrow) along which water bodies subjected to evaporation evolve. Deviation from the GMWL is quantified by the D-excess parameter. B). Triple oxygen isotope hydrology. Most precipitation falls on the triple oxygen GMWL with slope of 0.528, while evaporating bodies of water follow a shallower slope. The deviation from the GMWL is quantified by the $\Delta^{17}O$ parameter. C). As for (B), but plotted as $\Delta^{17}O$ versus $\delta^{18}O$. D) Schematic depiction of the back projection method for reconstructing the $\delta^{18}O$ of unevaporated precipitation ($\delta^{18}O_{\text{rucp}}$). The dashed horizontal line is a characteristic meteoric water line, and the arrow is the evaporation slope, along which an evaporated water composition (black circle) is projected to its intercept with the meteoric water line.

from the GMWL is referred to as the *deuterium-excess* (or *d-excess*), and defined by the deviation from the slope 8 line:

$$d\text{-excess} = \delta D - 8 * \delta^{18}O \quad \text{Equation 2}$$

d-excess is extensively used as an indicator of evaporatively-modified water bodies in the present-day, but its application into the paleo-record is limited by the lack of suitable authigenic minerals that record both the hydrogen and oxygen isotope composition of the waters in which they form.

A major benefit of triple oxygen isotopes is that the $^{17}\text{O}/^{16}\text{O}$ ratio serves a function analogous to the $^2\text{H}/^1\text{H}$ ratio in terms of sensitivity to evaporation (Figure 2B), so any authigenic oxygen-bearing mineral can potentially record information about evaporation. ^{17}O has been overlooked until recently, in part because the mass-dependent fractionation ratio between $^{17}\text{O}/^{16}\text{O}$ and $^{18}\text{O}/^{16}\text{O}$ for equilibrium versus kinetic fraction was not resolvable with existing analytical techniques. Improvements in the analytical precision of simultaneous $^{17}\text{O}/^{16}\text{O}$ and $^{18}\text{O}/^{16}\text{O}$ measurements of waters (Baker et al., 2002; Barkan and Luz, 2005) has allowed for clear identification of such differences. These differences are quantified by the fractionation exponent θ , where:

$$\theta = \frac{\ln\left(\frac{^{17}/^{16}\alpha}{^{18}/^{16}\alpha}\right)}{\ln\left(\frac{^{17}/^{16}\alpha}{^{18}/^{16}\alpha}\right)} \quad \text{Equation 3}$$

The fractionation exponent for equilibrium fractionation between water vapor and liquid water is 0.528 (Barkan and Luz, 2005), whereas the value for diffusion of water vapor through air (the kinetic aspect of evaporation) is 0.5185 (Barkan and Luz, 2007). Therefore, analogous to the δD to $\delta^{18}\text{O}$ system, waters mostly influenced by equilibrium fractionation will plot with a slope close to 0.528 in a plot of $\delta^{17}\text{O}$ versus $\delta^{18}\text{O}$, and those influenced by evaporation will track along a lower slope [where $\delta' =$

$\ln(R_{\text{sample}} / R_{\text{standard}})$]. Analogous to d-excess, the parameter $\Delta^{17}\text{O}$ is a measure of the deviation from a reference line with a slope of 0.528 (Figure 2C):

$$\Delta^{17}\text{O} = \delta^{17}\text{O} - 0.528 * \delta^{18}\text{O} \quad \text{Equation 4}$$

where

$$\delta^{1x}\text{O} = \ln\left[\frac{{}^{1x}R_{\text{sample}}}{{}^{1x}R_{\text{standard}}}\right] \quad \text{Equation 5}$$

and $1x = 17$ or 18 .

Evaporation causes a lowering of the $\Delta^{17}\text{O}$ value of the residual waters, and this has been documented in studies of modern lakes (Surma et al., 2015, 2018; Gázquez et al., 2018; Passey and Ji, 2019). High-precision triple oxygen isotope analysis of carbonate minerals is now possible (Passey et al., 2014; Barkan and Luz, 2015; Wostbrock et al., 2020), enabling the study of triple oxygen isotopes in a variety of settings, including carbonate-producing lakes. Triple oxygen isotopes promise to shed light on the nature of down-core isotopic variation in lacustrine carbonates. Changes in regional climate and the extent of prior Rayleigh distillation of moisture sources should result in arrays of data with a slope of 0.528 in $\Delta^{17}\text{O} - \delta^{18}\text{O}$ space and relatively high $\Delta^{17}\text{O}$ values, whereas changes in the extent of evaporation of lakes should result in slopes of 0.524 ± 0.002 and low $\Delta^{17}\text{O}$ values (Passey and Ji, 2019).

In addition, Passey and Ji (2019) explored a method for reconstructing the pre-evaporated $\delta^{18}\text{O}$ value of lake catchment precipitation (so-called reconstructed unevaporated catchment precipitation, or RUCP). Reconstructing this parameter is important because of the climate signal that is contained in $\delta^{18}\text{O}$ of precipitation (e.g., Craig, 1961; Dansgaard, 1964; Gat, 1996). The method involves back projection in $\Delta^{17}\text{O} - \delta^{18}\text{O}$ space from the evaporated water composition along a slope characteristic of evaporation to the intersection with the triple oxygen isotope meteoric water line (Figure 2D). The method requires an assumption about the $\Delta^{17}\text{O}$ of the paleo-meteoric water line and rests on the observation that the evaporation slope is fairly uniform across the range of modern lake systems that have been studied. In this study, we will use the approach of Passey and Ji (2019) to place constraints on the degree of variation in the isotopic composition of precipitation falling in Bear Lake's catchment over the past ~25 ka.

Clumped Isotope Thermometry

Clumped isotope thermometry is based on the temperature-dependent ‘clumping’ of heavy isotopes within the same molecule (Wang et al., 2004; Schauble et al., 2006; Ghosh et al., 2006). In the case of carbonate minerals, the ^{13}C - ^{18}O isotope clump found in the $\text{Ca}^{13}\text{C}^{18}\text{O}^{16}\text{O}_2$ isotopologue has received the most study. Excess in ^{13}C - ^{18}O clumping is described by the Δ_{47} parameter, which is a measure of excess isotopic clumping measured in CO_2 produced by phosphoric acid digestion of carbonate minerals:

$$\Delta_{47} = \frac{{}^{47}R_{\text{sample}}}{{}^{47}R_{\text{stochastic}}} - 1 \quad \text{Equation 6}$$

where ${}^{47}R_{\text{sample}}$ is the abundance ratio of mass 47 CO_2 (primarily $^{13}\text{C}^{18}\text{O}^{16}\text{O}$) to mass 44 CO_2 ($^{12}\text{C}^{16}\text{O}_2$) for a sample, and ${}^{47}R_{\text{stochastic}}$ is the same abundance ratio, but for CO_2 with identical bulk isotopic composition ($^{13}\text{C}/^{12}\text{C}$, $^{17}\text{O}/^{16}\text{O}$, $^{18}\text{O}/^{16}\text{O}$) as the sample, but with levels of $^{13}\text{C}^{18}\text{O}^{16}\text{O}$ expected for stochastic combinations of isotopes (i.e., with no thermodynamic excess in ^{13}C - ^{18}O clumping). Dozens of calibration equations between Δ_{47} and carbonate growth temperature have been published (see Petersen et al., 2019), but only two studies have examined authigenic lacustrine carbonates in detail (Huntington et al. 2010; Li et al., 2021). Data from both studies demonstrate that Δ_{47} values of lacustrine carbonates track summertime surface water temperatures and show no significant differences in Δ_{47} between aragonite-dominant and calcite-dominant mineralogies. In this study we use the calibration equation of Petersen et al., (2019) to calculate formation temperature from measured Δ_{47} values [$T(\Delta_{47})$], recognizing that this temperature most likely (but not necessarily) reflects summertime water temperatures, which in turn can be related to air temperature including mean annual air temperature (Hren and Sheldon, 2012).

Detrital carbonate in lakes is commonly sourced from nearby rock units containing marine limestones and dolomites. These commonly have high $T(\Delta_{47})$ values ($> 50\text{ }^\circ\text{C}$) that do not reflect original water temperatures, but instead result from recrystallization or solid-state isotopic reordering while the

rock units experienced elevated temperatures during burial (e.g., Ferry et al., 2011; Shenton et al., 2015; Bergmann et al., 2018; Ryb et al., 2021). This property makes clumped isotopes particularly sensitive to detrital contamination, because the detrital $T(\Delta_{47})$ is well outside of the range for authigenic lacustrine carbonates, whereas detrital $\delta^{13}\text{C}$ and $\delta^{18}\text{O}$ values may overlap authigenic compositions.

Bear Lake

Bear Lake is located along the Utah / Idaho border (Figure 1), and is a moderately alkaline lake that is roughly 32 km long and 6 to 13 km wide with a mean depth of 28m (Dean et al., 2006). Bear Lake resides in an intermontane fault-block graben with a present surface elevation of 1802 m, bounded by the Bear River Range on the west (maximum elevation 3030 m) and the Bear Lake Plateau on the east (maximum elevation 2270 m). It is home to endemic ostracods and fish species, and is used by humans for recreation, and for agricultural and municipal water storage (Dean et al., 2006; Dean, 2009). Bear Lake's main inflows include several small creeks draining the Bear River Range, as well as the Bear River, sourced from the northeastern Uinta Mountains. Bear River has alternated between being connected and disconnected from the lake in the past, and is presently connected through a series of controlled diversion canals that allow the lake to function as a reservoir for Bear River water (Dean et al., 2006; Dean, 2009) (Figure 1).

In September 2000, the Global Lake Drilling to 800 meters (GLAD800) program retrieved two adjacent cores from the lake of 100 m and 120 m length. The core site average linear sedimentation rate of 0.54 mm/yr^{-1} shows minor variation through time (Kaufman et al., 2009). Carbonate mineralogy and abundances determined by Rosenbaum and Heil (2009) suggest fluctuating periods of open and closed lake system dynamics. Periods of high carbonate abundance (as aragonite) are correlated with interglacials (Holocene, Marine Isotope Stage (MIS) 5e, MIS 7), and are interpreted to correspond to a closed lake system where Bear River was disconnected from the lake and outflow was minimal or nonexistent. Periods of low carbonate abundance characterize most of the core, and suggest increased

detrital influence from Bear River and creeks from the adjacent Bear River Mountains and Bear Lake Plateau, within a fresh-water flow-through lake system.

Stable isotope values measured on bulk carbonate show a distinct positive $\delta^{18}\text{O}$ shift (>5 per mil) moving from the LGM to the Holocene that correspond to the shift to high carbonate abundance (Figure 1) (Bright et al., 2006; Kaufman et al., 2009). Bear Lake is an ideal test locality to determine if the high $\delta^{18}\text{O}$ carbonates that formed during putative closed lake basin conditions in fact have a higher evaporative signal (low $\Delta^{17}\text{O}$) than the LGM portion of the core, and whether clumped isotope analyses reveal the extent to which the measured isotopic compositions are influenced by detrital carbonate.

MATERIALS AND METHODS

Core Samples and Age Model

We obtained 25 samples from core BL00-1E spanning 0.2 to 15 meters below lake floor (mblf) from the LacCore facility. The samples derive from two lithostratigraphic units, an upper aragonitic marl (0 to ~8.5 mblf, or approximately 0 to 11.4 ka), and a lower silty clay (below ~8.5 m, or 11.4 to 24.6 ka) (Kaufman et al., 2009). The upper aragonitic marl is carbonate-rich (~60 – 80%) and dominated by aragonite with minor dolomite (~5%) and calcite (~10%). Aragonite disappears abruptly in the lower silty clay, which contains ~15 – 20% calcite and 5 – 10% dolomite. These estimates are based on x-ray diffraction peak intensities and therefore are qualitative estimates of mineral weight percent (Kaufman et al., 2009).

We use the age model from Colman et al. (2009), accessed from <https://www.ncei.noaa.gov/access/paleo-search/study/8648>. It is based on radiocarbon ages from the core, as well as radiocarbon ages from other Bear Lake cores that were transferred to BL00-1 on the basis of magnetic susceptibility correlations. It is important to note that gaps in age control exist from 3.4 ka to the core top (assumed to be 0 ka), and from 14.6 to 26.5 ka. For the latter, the sedimentation rate is

comparable to that of the younger portion of the core, and ^{14}C dates from correlative units in other Bear Lake cores are stratigraphically ordered. Therefore, the chronology for this interval is probably reliable as a first approximation, but caution should be used if comparing details from BL00-1 / 1E proxy data to absolute-dated records (e.g., U-Th dated speleothem records).

Sample preparation

Subsamples of each core sample were gently disaggregated using a mortar and pestle, and then treated to remove labile organics using 3% hydrogen peroxide (H_2O_2), rinsed 3 times with deionized water, centrifuged for 5-10 minutes between rinses, decanted, and dried overnight at 50 °C. Treated sample powders were homogenized and stored in glass vials prior to isotopic measurements. Each triple oxygen and clumped isotope analysis required 8-100 mg of sample material, depending on carbonate weight percent, where 6-8 mg is necessary for pure carbonate.

Clumped isotope analysis

Clumped isotope (Δ_{47}) analyses of carbonates were conducted using a Nu Perspective-IS dual inlet isotope ratio mass spectrometer (instrument PS021). Sample CO_2 was prepared for mass spectrometry using methods described in Passey et al. (2010). Briefly, carbonates were digested in 100% phosphoric acid (H_3PO_4) at 90 °C in a common acid bath (CAB), or at 25-50 °C in sealed two-leg vessels. Gas was purified by passage through cryogenic traps and a Porapak-Q packed gas chromatography column held at -20 °C. CO_2 isotopologues of interest (mass 44-49) were measured at an ion current of 40 nano Amps (nA) for the major ion beam across 40 sample gas/reference gas cycles, where each cycle has an idle time of 20 seconds (s) and an integration time of 50s for each gas (= total integration time of 2000s for each gas).

Triple oxygen isotope analysis

Triple oxygen isotope ($\delta^{17}\text{O}$, $\delta^{18}\text{O}$) analyses of carbonates were conducted using the acid digestion-methanation-fluorination of Passey et al. (2014). Treated carbonate samples, 8-80 mg, were digested in 100% H_3PO_4 at 90 °C in a CAB. The resulting CO_2 was reacted with H_2 over an iron catalyst at 560 °C to produce CH_4 and H_2O . The resulting H_2O was fluorinated at 360°C using cobalt trifluoride producing the oxygen (O_2) gas analyte for mass spectrometry, which was purified by passage through metal loops immersed in liquid nitrogen, and through a molecular sieve (5Å) gas chromatography column held at -78 °C. Temperature-stepped acid digestion at 25 and 50 °C was later implemented on samples with mixed carbonate composition with the resulting CO_2 processed using the same system, except with the acid reaction taking place in sealed two-leg vessels. Water samples were fluorinated using the same CoF_3 reactor, with the resulting O_2 purified in the same manner as the carbonate derived O_2 . The triple isotope composition of the O_2 was measured using a Nu Perspective-IS mass spectrometer (instrument PS022) at a major ion beam intensity of 20nA. Analyses were conducted across 40 reference cycles, with a 20s idle time and 50s integration time.

Temperature stepped reactions

Following initial clumped isotope measurements that revealed unrealistically high clumped isotope temperatures for the older calcitic / dolomitic portion of the core, selected samples were analyzed using temperature stepped acid digestion, at 25 °C and 50 °C. The 25 °C reactions were generally 45 minutes long and 50 °C reactions were 2 hours long. In this approach, carbon dioxide (CO_2) evolved from the 25 °C step is expected to result primarily from acid digestion of the more labile authigenic component (calcite or aragonite), whereas CO_2 evolved from the second, longer 50 °C step would

originate from the more refractory detrital dolomite component (if present) that resisted acid digestion in the initial 25 °C step (Degens and Epstein, 1964; Liu et al., 2019). This approach is imperfect, since it is generally not possible to achieve complete separation of mineral components (e.g., Liu et al., 2019), but it should be the case that the brief, low temperature step is more reflective of the aragonite / calcite component(s) and the longer, high temperature step is more reflective of the dolomite component.

These stepped acid digestions, performed in standard two-leg sealed vessels (SV), were used for both clumped and triple oxygen isotope measurements. For the latter, the evolved CO₂ was cryogenically extracted and purified using an offline vacuum extraction line, and then flame sealed in fused silica tubes for later analysis. For the clumped isotope measurements, the SV was attached directly onto the online gas clean-up line via flexible metal tubing and Swagelock UltraTorr fittings. A SV, or silica tube, was pumped down to background vacuum pressure of $\sim 10^{-3}$ mbar for 40 minutes before sample gas was introduced into the cryogenic clean-up line. Following introduction of the gas, the samples were processed in exactly the same manner as for the 90 °C common acid bath extractions.

Data correction and normalization

Clumped isotope data normalization

Clumped isotope analyses of lake sediments were conducted between December 2018 and December 2021 in 5 different sessions, termed Sessions A, B, C, D, and E. In general, several heated gases (1000°C), equilibrated gases (30°C), ETH carbonate standards, and other secondary carbonate standards such as NBS-19, IAEA-C1 and 102-GC-AZ01 were measured in each session.

Data were normalized based on a combined CO₂ equilibrium scale (Dennis et al., 2011) + ETH normalization using CO₂ equilibrated at 30 °C ($\Delta_{47} = 0.89407\text{‰}$ and $\Delta_{48} = 0.326\text{‰}$) and CO₂ heated at 1000 °C ($\Delta_{47} = 0.02659\text{‰}$ and $\Delta_{48} = -0.001\text{‰}$) (Petersen et al. 2019), ETH-1/ 2 ($\Delta_{47} = 0.20685\text{‰}$ and Δ_{48}

= 0.140‰), and ETH-3 ($\Delta_{47} = 0.61320\text{‰}$ and $\Delta_{48} = 0.299\text{‰}$) (Bernasconi et al., 2021). The pooled weighted average slope for the equilibrated gas line, heated gas line, and ETH-1/2 line were used to correct for linearity prior to application of a transfer function relating these linearity-corrected ‘raw’ Δ_{47} values to the accepted values reported above.

Clumped isotope temperatures of the carbonates [$T(\Delta_{47})$] were calculated using equation 1 from Peterson et al. (2019). The stepped-temperature reaction subset of samples reacted at 25 and 50 °C require a correction for acid temperature prior to calculation of $T(\Delta_{47})$. A value of 0.038 was added to samples reacted at 50 °C (Defliese et al. 2015) and a value of 0.0831 was added to the 90 °C measurements to account for the temperature dependent acid fractionation (Peterson et al. 2019). Thus, data are reported as 25 °C acid-reaction-temperature Δ_{47} values, and an offset value was not necessary for samples reacted at 25 °C.

Triple oxygen isotope data normalization

Triple oxygen isotope data were normalized to the VSMOW-SLAP scale using concurrent analyses of VSMOW and SLAP (typically 8 analyses of each per session, analyzed in blocks of 3-4 replicates). Data are first normalized to VSMOW ($\delta^{18}\text{O}$, $\delta^{17}\text{O}$, and $\Delta^{17}\text{O} = 0\text{‰}$), and then scaled to SLAP ($\delta^{18}\text{O} = -55.5\text{‰}$, $\delta^{17}\text{O} = -29.6986\text{‰}$) (Schoenemann et al., 2013).

Normalization of carbonate data involves three additional steps. First, $\delta^{18}\text{O}$ values are corrected following the observation (e.g., Passey et al., 2014) of a consistent offset between $\delta^{18}\text{O}$ values measured in O_2 from this method (acid digestion - methanation - fluorination) and ‘known’ $\delta^{18}\text{O}$ values measured using traditional acid digestion and mass spectrometry of CO_2 . To perform this correction, we use a linear regression between $\delta^{18}\text{O}(\text{O}_2)$ and $\delta^{18}\text{O}(\text{CO}_2)$ for analyses where the latter have been determined (including both carbonate standards and unknowns). The analogous correction for $\delta^{17}\text{O}$ is based on the

magnitude of the $\delta^{18}\text{O}$ correction assuming a mass dependency of 0.528 (i.e., the correction does not change the $\Delta^{17}\text{O}$ value).

Second, $\delta^{18}\text{O}$ values must be corrected for acid fractionation (because the oxygen in the O_2 that we analyze ultimately comes from CO_2 produced by acid digestion of carbonates). To do this, we apply a temperature dependent acid fractionation factor ($^{18}\alpha_{\text{acid}}$) of 1.00813, 1.00936, and 1.0130 for calcite (90 °C, 50 °C, and 25 °C reaction temperatures, respectively) and 1.00854, 1.00971, and 1.01060 for aragonite, as determined by Kim et al. (2007a).

Analogous corrections must be made for $\delta^{17}\text{O}$, but to-date there are no published values for the temperature-dependency of θ_{acid} , which allows for calculation of $^{17}\alpha_{\text{acid}}$ based on knowledge of $^{18}\alpha_{\text{acid}}$:

$$\theta_{\text{acid}} = \frac{\ln(^{17}\alpha_{\text{acid}})}{\ln(^{18}\alpha_{\text{acid}})} \quad \text{Equation 7}$$

We determined the temperature dependency of θ_{acid} by analyzing IAEA-603 and IAEA-C1 using our acid digestion–methanation–fluorination method with acid reaction temperatures of 90°C and 25°C. This procedure allows for measurement of $\delta^{17}\text{O}$ and $\delta^{18}\text{O}$ of CO_2 gas evolved during acid digestion (measured as O_2 following the methanation and fluorination steps), which can then be combined with the absolute mineral $\delta^{17}\text{O}$ and $\delta^{18}\text{O}$ values of IAEA-603 determined using direct BrF_5 fluorination by Wostbrock et al. (2020) to determine fractionation factors:

$$^{1x}\alpha_{\text{acid}} = \frac{1000 + \delta^{1x}\text{O}_{\text{gas}}}{1000 + \delta^{1x}\text{O}_{\text{mineral}}} \quad \text{Equation 8}$$

Where $1x = 17$ or 18 . Note that we pool gas analyses of IAEA-603 and IAEA-C1, as these reference materials come from a common stock and we have found them to be isotopically indistinguishable (Huth et al., 2022). We find no resolvable difference in θ_{acid} between 90 °C ($\theta_{\text{acid}} = 0.5223 \pm 0.0005$ 1 SEM) and 25 °C ($\theta_{\text{acid}} = 0.5223 \pm 0.0003$) acid digestions (Table 1). We assume

that the θ_{acid} for our intermediate reaction temperature of 50 °C is between the 90 °C and 25 °C values (i.e., also 0.5223). The value for 90 °C is indistinguishable from the value for 90 °C that we recently reported (Huth et al., 2022; 0.5224), and we therefore use this prior value for all acid temperatures in our data normalizations to avoid the introduction of multiple correction factors. IAEA-603 / IAEA-C1 is calcite, and we assume that the lack of significant temperature sensitivity in θ_{acid} is also true for aragonite, which is likely given the similarity in temperature response of $^{18}\alpha_{\text{acid}}$ between calcite and aragonite.

Finally, note in Table 1 that the $^{18}\alpha_{\text{acid}}$ values are highly variable compared to values that could be determined directly for CO₂ released by acid digestion (c.f., Kim et al., 2007a). This is expected given the relatively poor precision of the acid digestion – methanation – fluorination method for $\delta^{18}\text{O}$ (and $\delta^{17}\text{O}$) analysis. However, the fractionation effects leading to this poor precision are highly mass-dependent (Passey et al., 2014), which allows the acid digestion – methanation – fluorination method to have excellent precision in $\Delta^{17}\text{O}$ and, similarly, θ . Accordingly, we combine our precise measurements of θ_{acid} with the precise measurements of $^{18}\alpha_{\text{acid}}$ by Kim et al. (2007a) to calculate $^{17}\alpha_{\text{acid}}$ values using Equation 7. For calcite, these $^{17}\alpha_{\text{acid}}$ values are 1.004238, 1.004880, and 1.005369 (90 °C, 50 °C, and 25 °C, respectively), and for aragonite they are 1.004453, 1.005059, and 1.005521.

Calculation of paleo-lake water isotopic composition

Paleo-lake water oxygen isotopic composition (i.e., carbonate ‘parent waters’) can be calculated based on measured carbonate data ($\delta^{18}\text{O}$ and $\Delta^{17}\text{O}$), given knowledge of the temperature-dependent mineral-water fractionation factors. For $^{18}\alpha_{\text{mineral-water}}$, we used the Kim and O’Neil (1997) calcite-water fractionation factor equation: $1000 \ln ^{18}\alpha = 18030/ T - 32.42$, and the Kim et al. (2007b) aragonite-water equation: $1000 \ln ^{18}\alpha = 17880/ T - 31.14$. We calculated the corresponding $^{17}\alpha_{\text{mineral-water}}$ using our

Table 1. Triple oxygen isotope acid fractionation factors for 25 °C sealed vessel reactions and 90 °C common acid bath reactions, relative to the $\delta^{17}\text{O}$ and $\delta^{18}\text{O}$ values of IAEA-603 mineral reported by Wostbrock et al. (2020).

Sample ID	Lab Number	Analytical Session	Reaction Time (hr)	$\delta^{17}\text{O}(\text{O}_2/\text{CaCO}_3)$ VSMOW-SLAP	$\delta^{18}\text{O}(\text{O}_2/\text{CaCO}_3)$ VSMOW-SLAP	$^{17}\alpha_{\text{gas-mineral}}$	$^{18}\alpha_{\text{gas-mineral}}$	$\theta_{\text{gas-mineral}}$
<i>25 °C sealed vessel reactions</i>								
IAEA-C1	3120-R18-1	18	1	20.234	38.963	1.0053236	1.0102030	0.5230
IAEA-C1	3121-R18-1	18	18.5	20.568	39.602	1.0056536	1.0108236	0.5237
IAEA-C1	3225-R18-2	18	18.5	19.505	37.555	1.0046053	1.0088334	0.5224
IAEA-C1	3225-R18-3	18	18.5	20.522	39.531	1.0056079	1.0107548	0.5228
IAEA-C1	3264-R19-1	19	3	19.851	38.251	1.0049465	1.0095104	0.5213
IAEA-C1	3265-R19-2	19	3	19.196	36.993	1.0043015	1.0082873	0.5201
IAEA-C1	3279-R19-3	19	1	19.884	38.321	1.0049794	1.0095781	0.5211
IAEA-603	3292-R19-1	19	18.7	20.220	38.925	1.0053106	1.0101659	0.5237
							Average	0.5223
							Std. Error	0.0005
<i>90 °C common acid bath reactions</i>								
IAEA-C1	2990-R18-1	18	0.17	18.788	36.145	1.0038991	1.0074629	0.5234
IAEA-C1	2991-R18-2	18	0.17	19.659	37.838	1.0047571	1.0091084	0.5234
IAEA-603	2992-R18-1	18	0.17	19.842	38.175	1.0049382	1.0094367	0.5245
IAEA-C1	3108-R18-3	18	0.17	19.329	37.199	1.0044325	1.0084876	0.5233
IAEA-C1	3109-R18-4	18	0.17	19.782	38.085	1.0048785	1.0093486	0.5230
IAEA-603	3110-R18-2	18	0.17	18.925	36.434	1.0040344	1.0077436	0.5220
IAEA-C1	3119-R18-5	18	0.17	19.074	36.735	1.0041805	1.0080364	0.5212
IAEA-603	3209-R18-5	18	0.17	19.469	37.498	1.0045698	1.0087778	0.5217
IAEA-C1	3224-R18-9	18	0.17	19.436	37.425	1.0045373	1.0087073	0.5222
IAEA-C1	3259-R19-3	19	0.17	19.095	36.752	1.0042013	1.0080528	0.5227
IAEA-C1	3260-R19-4	19	0.17	19.314	37.155	1.0044171	1.0084443	0.5241
IAEA-603	3262-R19-1	19	0.17	19.139	36.843	1.0042452	1.0081413	0.5225
IAEA-C1	3279-R19-8	19	0.17	18.563	35.773	1.0036778	1.0071006	0.5188
IAEA-603	3284-R19-2	19	0.17	18.590	35.801	1.0037041	1.0071280	0.5205
IAEA-C1	3286-R19-9	19	0.17	19.382	37.333	1.0044848	1.0086174	0.5215
IAEA-603	3293-R19-3	19	0.17	19.493	37.527	1.0045939	1.0088066	0.5227
IAEA-C1	3294-R19-10	19	0.17	18.963	36.528	1.0040711	1.0078348	0.5206
IAEA-C1	3295-R19-11	19	0.17	19.406	37.346	1.0045080	1.0086299	0.5234
							Average	0.5223
							Std. Error	0.0003
<i>Mineral isotopic composition (Wostbrock et al., 2020)</i>								
IAEA-603				14.831	28.470	($\Delta^{17}\text{O} = -100$ per meg)		

updated triple oxygen mineral-water fractionation value of $\theta = 0.5250$ from Huth et al. (2022). For temperature, we use the temperatures inferred from clumped isotope thermometry [$T(\Delta_{47})$], or if $T(\Delta_{47})$ values are deemed unreliable (i.e., resulting from detrital carbonate contamination), we make assumptions about carbonate formation temperatures, as described in the discussion section. We use a Monte-Carlo approach to account for uncertainty in mineral isotopic compositions, fractionation factors, and temperatures of formation. Specifically, parent water isotopic compositions are calculated 500 times using a Matlab script that randomly samples each parameter from a Gaussian distribution with mean equal to the measured value of the parameter, and standard deviation equal to the uncertainty in the parameter (typically as 1 S.E.M.). These uncertainties are given in the relevant tables, along with the mean and standard deviation of the 500 calculations of parent water isotopic composition for each sample.

Calculation of reconstructed unevaporated catchment precipitation

Combining $\Delta^{17}\text{O}$, Δ_{47} temperature, and calculated parent water values, we can identify and remove evaporative effects to determine pristine unevaporated catchment precipitation. The back projection method used follows Passey and Ji (2019) where:

$$\delta'^{18}\text{O}_{RUCP} = \frac{\Delta'^{17}\text{O}_{MWL} - \Delta'^{17}\text{O}_{lake} + (\lambda_{lake} - \lambda_{ref})\delta'^{18}\text{O}_{lake}}{\lambda_{lake} - \lambda_{ref}} \quad \text{Equation 9}$$

where λ_{lake} is calculated as a third-order polynomial of $\Delta'^{17}\text{O}_{lake}$:

$$\lambda_{lake} = 1.9856 \times (\Delta'^{17}\text{O}_{lake})^3 + 0.5730 \times (\Delta'^{17}\text{O}_{lake})^2 + 0.0601 \times \Delta'^{17}\text{O}_{lake} + 0.5236$$

Equation 10

The parameter $\Delta'^{17}\text{O}_{MWL}$ is the $\Delta'^{17}\text{O}$ of the meteoric water line that existed at the time of carbonate formation. This parameter is unconstrained, and the RUCP calculation rests on the assumption that $\Delta'^{17}\text{O}_{MWL}$ does not vary substantially through time. In this study, we use $\Delta'^{17}\text{O}_{MWL} = 0.027\text{‰}$, which is

present-day average $\Delta^{17}\text{O}$ of precipitation in the western United States (Kelson et al. 2022), and we apply an uncertainty of $\pm 0.005\text{‰}$ to this value. Like the calculation of parent water isotopic composition, we use a Monte-Carlo sampling approach to incorporate error associated with uncertainty in parent water isotopic composition ($\delta^{18}\text{O}_{\text{lake}}$, $\Delta^{17}\text{O}_{\text{lake}}$), the evaporation slope λ_{lake} , and the $\Delta^{17}\text{O}$ of unevaporated meteoric water ($\Delta^{17}\text{O}_{\text{MWL}}$), with error values reported in the relevant tables.

RESULTS

Isotopic compositions of Bear Lake carbonates and surrounding bedrock are reported in Tables 2 and 3 and are displayed in Figure 3. Temperatures inferred from clumped isotope thermometry (Figure 3A) average $85 \pm 16\text{ °C}$ (1σ) for local bedrock, $17 \pm 5\text{ °C}$ for the upper aragonitic portion of the core (Holocene), and $40 \pm 12\text{ °C}$ for the lower calcitic / dolomitic (late glacial) portion of the core (when 90 °C phosphoric acid digestion was used). When 25 °C phosphoric acid digestions are used for the lower portion (which should selectively react calcite over dolomite), $T(\Delta_{47})$ values decrease to $31 \pm 9\text{ °C}$, and when the unreacted residual material from 25 °C reactions is subsequently reacted at 50 °C , $T(\Delta_{47})$ values increase to $50 \pm 5\text{ °C}$.

Similar patterns are seen for $\delta^{13}\text{C}$ (Figure 3B), $\delta^{18}\text{O}$ (Figure 3C), and $\Delta^{17}\text{O}$ values (Figure 3D). With few exceptions, values resulting from 25 °C acid digestions are most dissimilar to the isotopic compositions of bedrock, those from 50 °C reactions are most similar, and those from 90 °C reactions—which did not have a prior 25 °C extract as did the 50 °C reactions—are intermediate. The pattern is least clear for $\Delta^{17}\text{O}$, which shows significant overlap between the isotopic composition of bedrock and lake core carbonate.

Table 2. Clumped isotope results for GLAD1-BL00-1E core samples and local bedrock. Data are reported in per mil relative to a hybrid carbon dioxide equilibrium scale / ETH Zurich scale (CDES/ETH). The sample ID indicates the temperature used for phosphoric acid digestion.

Sample ID*	Depth (mblf)	Model Age (ka)	N (analyses)	$\delta^{13}\text{C}$ (‰) (VPDB)	$\delta^{18}\text{O}$ (‰) (VPDB)	Δ_{47} CDES/ETH (as measured)	Δ_{47} CDES/ETH (as 25°C rxn)	Δ_{47} CDES/ETH (1 SEM)	T Δ_{47} (°C)	T Δ_{47} (1 SEM)
Upper aragonitic section										
1H-1-20 90C	0.2	0.2	4	2.6	-4.6	0.647	0.735	0.013	10.4	3.7
1H-1-50 90C	0.5	0.5	3	3.0	-3.8	0.646	0.734	0.010	10.6	3.1
1H-2-80 90C	0.8	0.8	7	3.0	-3.8	0.637	0.725	0.007	13.4	2.1
1H-2-80 25C	0.8	0.8	3	3.0	-3.9	0.707	0.707	0.010	19.1	3.4
2H-1-220 90C	2.2	2.1	3	2.8	-4.0	0.654	0.742	0.010	8.3	3.0
2H-1-320 90C	3.2	3.1	3	2.4	-5.1	0.646	0.734	0.010	10.7	3.1
2H-1-370 90C	3.7	3.6	3	2.6	-4.7	0.625	0.713	0.015	17.2	4.8
2H-1-440 90C	4.4	4.4	3	2.4	-5.5	0.628	0.716	0.010	16.2	3.1
3H-1-550 90C	5.5	5.6	3	2.6	-4.6	0.604	0.692	0.010	24.0	3.6
3H-1-590 90C	5.9	6.1	2	2.3	-5.0	0.615	0.703	0.010	20.8	3.4
3H-1-660 90C	6.6	7.2	3	2.1	-5.7	0.603	0.691	0.018	24.5	6.1
3H-2-715 90C	7.15	8.2	3	0.4	-7.8	0.616	0.704	0.010	19.8	3.4
3H-2-800 90C	8	10.1	3	3.0	-4.5	0.610	0.698	0.010	21.9	3.5
Lower calcitic / dolomitic section										
4H-1-860 90C	8.6	11.6	3	1.2	-6.8	0.608	0.696	0.010	22.5	3.5
4H-1-925 90C	9.25	13.4	3	-1.0	-10.6	0.624	0.712	0.010	17.3	3.3
4H-2-A-1026 90C	10.26	16.0	1	-1.6	-7.5	0.524	0.612	0.018	55.9	8.4
4H-2-A-1026 50C	10.26	16.0	2	-1.6	-6.4	0.592	0.630	0.035	48.9	15.3
4H-2-A-1026 25C	10.26	16.0	2	-3.4	-8.4	0.708	0.708	0.024	19.0	7.8
4H-2-A-1060 90C	10.6	16.8	2	-2.2	-8.0	0.544	0.632	0.013	46.9	5.4
4H-2-A-1080 90C	10.8	17.2	1	-2.4	-8.6	0.571	0.659	0.018	36.0	7.0
5H-1-A-1120 90C	11.2	18.1	3	-2.8	-9.0	0.535	0.623	0.010	50.9	4.6
5H-1-A-1120 50C	11.2	18.1	2	-1.9	-6.9	0.592	0.630	0.013	47.9	5.5
5H-1-A-1120 25C	11.2	18.1	4	-3.4	-10.0	0.641	0.641	0.009	43.0	3.7
5H-1-A-1210 90C	12.1	20.0	1	-2.2	-8.6	0.587	0.675	0.018	30.1	6.6
5H-1-A-1245 90C	12.45	20.6	2	-1.8	-8.1	0.538	0.626	0.013	49.5	5.6
5H-1-A-1245 50C	12.45	20.6	1	-1.2	-6.1	0.566	0.604	0.018	59.7	8.7
5H-1-A-1245 25C	12.45	20.6	1	-2.5	-9.8	0.665	0.665	0.018	33.6	6.8
5H-2-A-1300 90C	13	21.6	6	-2.3	-8.5	0.556	0.644	0.008	42.2	3.3
5H-2-A-1300 50C	13	21.6	1	-1.4	-6.5	0.591	0.629	0.018	48.3	7.8
5H-2-A-1300 25C	13	21.6	3	-3.2	-9.8	0.667	0.667	0.010	32.9	3.9
5H-2-A-1320 90C	13.2	22.0	1	-2.1	-8.2	0.541	0.629	0.018	48.0	7.8
6H-1-A-1500 90C	15	24.6	6	-2.5	-9.1	0.557	0.645	0.007	41.6	3.0
6H-1-A-1500 50C	15	24.6	1	-1.6	-7.1	0.596	0.634	0.018	46.0	7.6
6H-1-A-1500 25C	15	24.6	3	-3.2	-10.1	0.678	0.678	0.010	29.0	3.7
Bedrock										
	<u>Formation</u>									
US21-UT-150	Fish Haven Dolomite									
US21-UT-151	Laketown Dolomite									
US21-UT-153	Hyrum Dolomite									
US21-UT-156	Thanynes Limestone									

*All core samples IDs have the prefix "GLAD1-BL00-1E", which has been omitted for clarity

Table 3. Triple oxygen isotope results for GLAD1-BL00-1E core samples and local bedrock. Data are reported relative to VSMOW-SLAP ($\lambda = 0.528$) as carbonate mineral, where $\Delta^{17}\text{O}$ of IAEA-603 = -0.100 ‰ (Wostbrock et al., 2020).

Sample ID*	Depth (mblf)	Model Age (ka)	n	$\delta^{18}\text{O}$	$\delta^{18}\text{O}$ (1 SEM)	$\Delta^{17}\text{O}$	$\Delta^{17}\text{O}$ (1 SEM)
Upper aragonitic section							
1H-2-80 90C	0.8	0.8	3	27.186	0.5	-0.117	0.006
1H-2-80 25C	0.8	0.8	4	26.272	0.4	-0.115	0.005
2H-1-220 90C	2.2	2.1	2	26.774	0.7	-0.124	0.007
2H-1-320 90C	3.2	3.1	2	25.855	0.6	-0.121	0.007
2H-1-440 90C	4.4	4.4	3	24.225	1.1	-0.109	0.011
3H-1-550 90C	5.5	5.6	2	26.510	0.6	-0.112	0.007
3H-1-660 90C	6.6	7.2	2	24.538	0.7	-0.113	0.007
3H-2-715 90C	7.15	8.2	3	22.747	0.5	-0.093	0.008
3H-2-800 90C	8	10.1	4	25.938	0.5	-0.115	0.009
Lower calcitic / dolomitic section							
4H-1-860 90C	8.6	11.6	2	23.019	0.6	-0.107	0.007
4H-2-A-1026 90C	10.26	16.0	2	21.069	1.3	-0.103	0.007
4H-2-A-1026 25C	10.26	16.0	1	21.210	0.8	-0.082	0.010
4H-2-A-1026 50C	10.26	16.0	2	25.085	0.6	-0.106	0.007
4H-2-A-1060 90C	10.6	16.8	2	23.310	0.6	-0.106	0.007
4H-2-A-1080 90C	10.8	17.2	4	21.373	0.8	-0.092	0.006
5H-1-A-1120 90C	11.2	18.1	2	22.325	0.6	-0.088	0.007
5H-1-A-1120 25C	11.2	18.1	2	20.149	0.6	-0.083	0.007
5H-1-A-1120 50C	11.2	18.1	4	23.627	0.4	-0.099	0.007
5H-1-A-1245 90C	12.45	20.6	2	23.008	0.6	-0.098	0.007
5H-1-A-1245 25C	12.45	20.6	1	21.914	0.8	-0.103	0.010
5H-2-A-1300 90C	13	21.6	2	22.702	0.6	-0.093	0.007
5H-2-A-1300 25C	13	21.6	4	20.178	0.4	-0.076	0.013
5H-2-A-1300 50C	13	21.6	4	23.579	0.6	-0.100	0.013
5H-2-A-1320 90C	13.2	22.0	2	22.405	0.6	-0.096	0.007
6H-1-A-1500 90C	15	24.6	4	22.699	0.4	-0.097	0.005
6H-1-A-1500 25C	15	24.6	1	20.430	0.8	-0.090	0.010
Bedrock							
		<u>Formation</u>					
US21-UT-150		Fish Haven Dolomite	2	26.745	0.6	-0.088	0.008
US21-UT-151		Laketown Dolomite	2	27.790	0.7	-0.096	0.007
US21-UT-153		Hyrum Dolomite	2	26.190	0.6	-0.106	0.010
US21-UT-156		Thanynes Limestone	2	24.341	0.6	-0.077	0.007

*All core samples IDs have the prefix "GLAD1-BL00-1E", which has been omitted for clarity

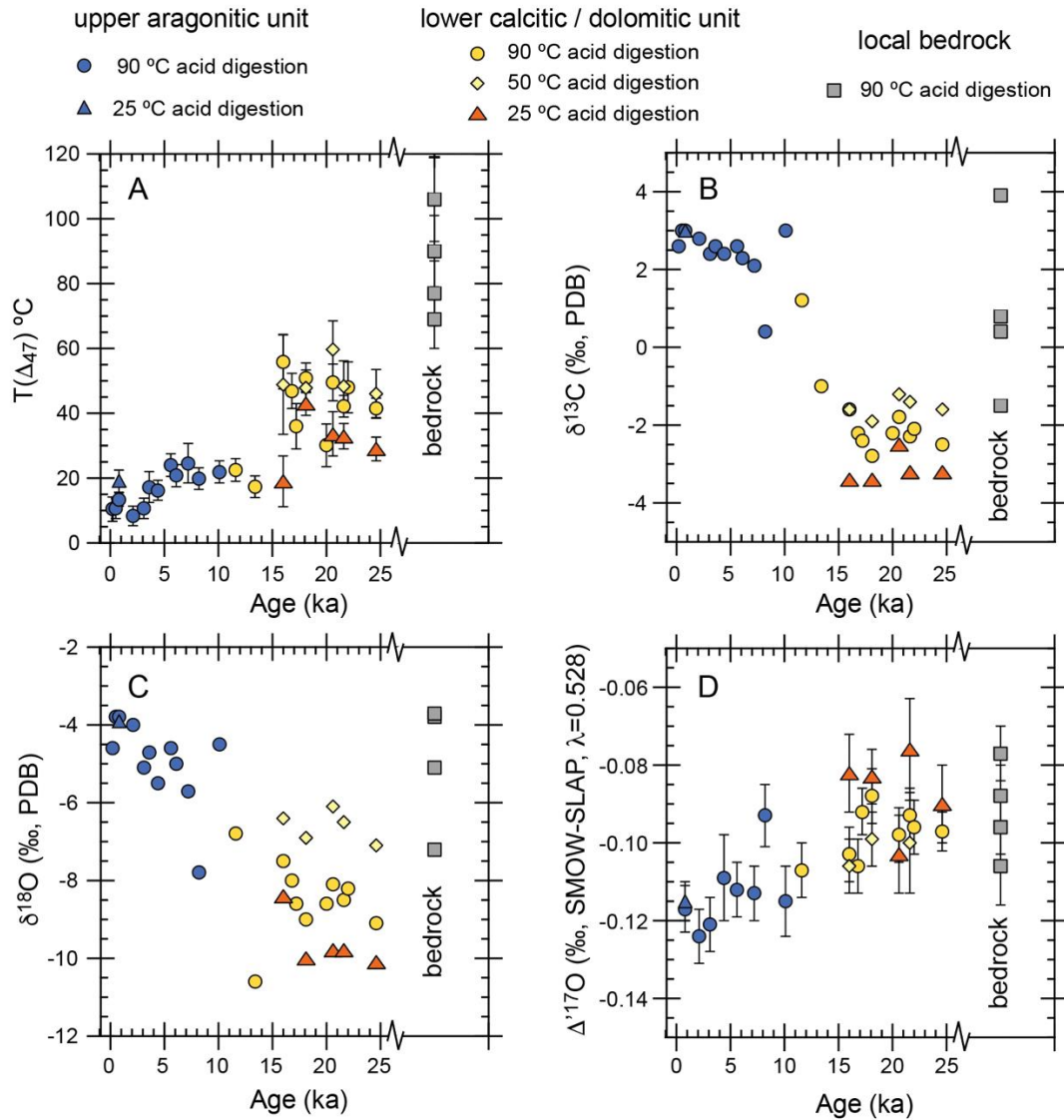


Figure 3. Stable isotope compositions of BL00-1E carbonates. (A) Temperatures inferred from clumped isotope thermometry. B) $\delta^{13}\text{C}$ values of carbonates. C) $\delta^{18}\text{O}$ values of carbonates. D) $\Delta^{17}\text{O}$ values of carbonates. For B and C, analytical error is smaller than the symbol size. For A and D, error bars are given as 1 SEM of the analytical uncertainty.

DISCUSSION

Detrital carbonate contamination

Detrital carbonate, including dolomite and possibly calcite, is known to be present in the Bear Lake sedimentary record (Bright et al., 2006; Kaufman et al., 2009). In the upper portion of the record where carbonate content is high, this detrital signal is swamped by the authigenic aragonite signal, whereas in the lower carbonate-poor portion of the record, the detrital signal may emerge. However, given that dolomite is less reactive in phosphoric acid than calcite or aragonite, it has been unclear how much influence this detrital component has had on measured isotopic compositions. The initial results to emerge from our study were from 90 °C acid digestions—which is the standard temperature used in our lab. The $T(\Delta_{47})$ values observed for the lower portion of the core, 40 ± 12 °C, are inconsistent with authigenic carbonate production in lacustrine environments, since lake water surface temperatures rarely exceed 30 °C, even in the hottest environments presently found on Earth (Hren and Sheldon, 2012). To find such temperatures at the latitudes of Bear Lake (42 °N) during the last glacial maximum is even less plausible.

Several observations are consistent with the hypothesis that detrital carbonate is the cause of the elevated $T(\Delta_{47})$ values in the lower portion of the record, as opposed to, e.g., isobaric contaminants interfering with mass spectrometry arising from volatile organics, sulfides, or other compounds found in lacustrine sediments. First, bedrock carbonate in the vicinity of Bear Lake has high $T(\Delta_{47})$ values, meaning that the presence of detrital carbonate would elevate $T(\Delta_{47})$ values of lake sediment. Second, selective reaction of lake sediment at 25 °C results in lower $T(\Delta_{47})$ values that are closer to plausible temperatures for authigenic calcite / aragonite mineralization, and reaction at 50 °C of the residual material from the 25 °C reactions yields $T(\Delta_{47})$ most similar to bedrock values. This is expected because the 25 °C reaction should selectively dissolve calcite / aragonite, leaving the residual fraction enriched in

recalcitrant carbonate, such as dolomite. Third, if detrital carbonate contributes significantly to the observed $T(\Delta_{47})$ of lake sediment, then its influence should be seen in the other, co-analyzed isotope systems ($\delta^{13}\text{C}$, $\delta^{18}\text{O}$, $\Delta^{17}\text{O}$). This influence is clearly observed for $\delta^{13}\text{C}$ and $\delta^{18}\text{O}$, where the results from 25 °C acid digestions are the most dissimilar and those from 50 °C reactions are most similar to bedrock compositions. The pattern is less clear for $\Delta^{17}\text{O}$, but this is not surprising given that the composition of bedrock overlaps the composition of lake sediment. Nevertheless, $\Delta^{17}\text{O}$ values from 25 °C reactions appear to be higher than those from higher temperature reactions, which suggests that the detrital composition is towards the lower end of the range observed for bedrock samples.

All of these observations are consistent with detrital carbonate having a strong impact on the measured isotopic compositions of lake sediment in the lower portion of the record. Detrital carbonate is not expected to have a major influence on the upper, aragonitic, carbonate-rich portion of the record given that the abundance of aragonite is ~10 times higher than that of dolomite (based on semiquantitative XRD data from Kaufman et al., 2009). Reaction of one aragonitic sample (1H-2-80) at 25 °C shows no appreciable difference in $\delta^{13}\text{C}$, $\delta^{18}\text{O}$, Δ_{47} , or $\Delta^{17}\text{O}$ compared to the same material reacted at 90 °C, which supports this expectation (Table 2 and 3).

An interpretive framework accounting for detrital carbonate contamination

Detrital carbonate significantly influences measured isotopic composition of lake sediments from the lower unit. This is true even for 25 °C acid digestions, where $T(\Delta_{47})$ values from the lower unit average 31 ± 9 °C, which is implausible for late glacial lake water temperatures. Therefore, we must regard all lower unit data from each isotope system studied as being influenced by detrital carbonate contamination. Despite this contamination, an interpretive framework can be developed that maximizes useful paleoclimate / paleoenvironmental information. This framework involves three elements.

First, we focus exclusively on data from 25 °C acid digestions from the lower core, as these are the least influenced by detrital carbonates. All interpretations of paleoclimate / paleohydrology moving forward are based on values from 25 °C reactions. For the upper aragonitic unit, we make use of the data from 90 °C reactions as well as the one sample reacted at 25 °C.

Second, given that the $T(\Delta_{47})$ values from the lower unit are unreliable, we calculate parent water isotopic compositions, which require an estimate of the temperature during carbonate mineralization, using three different scenarios: In Scenario 1, we use the measured $T(\Delta_{47})$ value from 25 °C reactions. Although these temperatures are generally implausible as actual authigenic carbonate growth temperatures, it is instructive to see how such temperatures influence calculations of parent water isotopic composition. In Scenario 2: we use the average $T(\Delta_{47})$ observed for the Holocene portion of the core (= 18 °C). Finally, in Scenario 3, we use a value 5 °C lower than the Holocene value (= 13 °C) as an approximation of the cooler climates that likely prevailed during the glacial (e.g, Seltzer et al., 2021; Osman et al., 2021).

Third, we interpret isotopic changes in terms of *lower limits* on the magnitude of change. Apart from the clumped isotope data, the presence of detrital carbonate reduces the apparent magnitude of isotopic change from the late glacial to the Holocene (Figure 3). For instance, in the $\delta^{13}\text{C}$ record (Figure 3B), the magnitude of change is +4.0‰ based on the 50 °C acid reaction data (= most detrital carbonate), +4.7‰ based on the 90 °C data (= a mixture of authigenic and detrital carbonate; this value excludes the samples from 11.6 and 13.4 ka which do not have 25 °C and 50 °C counterparts), and 5.6‰ based on the 25 °C data (least amount of detrital carbonate). Given that even the 25 °C data is not free of influence from detrital carbonate, the actual change in authigenic carbonate $\delta^{13}\text{C}$ from the late glacial to the Holocene must have been *at least* 5.6‰.

A final corollary to this third aspect is that we focus primarily on the magnitude of change between the pooled late glacial samples (25 to 15 ka) versus the pooled Holocene samples (10 ka to present). We do not view the higher-frequency variation within each time interval as being statistically

robust, owing to limits of analytical precision, and uncertainties in calculating parent water isotopic compositions and reconstructed unevaporated water isotopic compositions. Both of these factors are compounded by the low temporal resolution of the record.

Oxygen isotopic change in meteoric waters from the late glacial to the Holocene

Calculated isotopic compositions of carbonate parent waters (= lake waters) are reported in Table 4 and shown in Figure 4 for the three different temperature scenarios. Use of measured $T(\Delta_{47})$ values (Scenario 1) for lower unit sediments results in elevated apparent parent water $\delta^{18}\text{O}$ values and lower $\Delta^{17}\text{O}$ values. Use of the more realistic Scenario 2 ($T = 18\text{ }^\circ\text{C}$) or Scenario 3 ($T = 13\text{ }^\circ\text{C}$) leads to appreciably lower $\delta^{18}\text{O}$ values and higher $\Delta^{17}\text{O}$ values. If we consider Scenario 2 as an upper limit on actual lake water temperatures during the late glacial, then the shift in $\delta^{18}\text{O}$ from the late glacial to the Holocene was at least +4‰ (from $-8.6 \pm 0.7\text{‰}$ to $-4.6 \pm 1.5\text{‰}$). Likewise, the shift in lake water $\Delta^{17}\text{O}$ was at least -0.024 ‰ (from $0.002 \pm 0.011\text{‰}$ to $-0.022 \pm 0.008\text{‰}$). If actual glacial temperatures were 5 °C lower (Scenario 3), then the magnitude of the shifts would be 1‰ larger for $\delta^{18}\text{O}$ and 0.005‰ larger for $\Delta^{17}\text{O}$.

The inverse relationship between $\delta^{18}\text{O}$ and $\Delta^{17}\text{O}$ suggests that the major cause of isotopic change was an increase in the evaporative efflux from the lake following late glacial times. The triple oxygen isotope slope λ between glacial and Holocene time can be calculated as:

$$\lambda_{\text{glacial-Holocene}} = \frac{\delta^{17}\text{O}_{\text{glacial}} - \delta^{17}\text{O}_{\text{Holocene}}}{\delta^{18}\text{O}_{\text{glacial}} - \delta^{18}\text{O}_{\text{Holocene}}} \quad \text{Equation 11}$$

This value computes to $\lambda_{\text{glacial-Holocene}} = 0.522$. This value is characteristic of evaporation. For example, λ values relating highly evaporated western U.S. lakes and their (relatively) unevaporated source rivers range from 0.5219 to 0.5237 (Passey and Ji, 2019). Therefore, the triple oxygen isotope data are consistent with the glacial-Holocene $\delta^{18}\text{O}$ shift being driven largely if not entirely by a change in

Table 4. Calculated triple oxygen isotope compositions of carbonate parent waters and of reconstructed unevaporated catchment precipitation (RUCP), reported in per mil relative to VSMOW-SLAP with $\lambda = 0.528$ (Schonemann et al. 2013)

Sample ID§	Depth (m)	Model Age (ka)	N (analyses)	T Δ_{47} (°C)	mineral parent water isotopic compositions				RUCP	
					$\delta^{18}\text{O}$	$1\sigma^\ddagger$	$\Delta^{17}\text{O}$	$1\sigma^\ddagger$	$\delta^{18}\text{O}$	$1\sigma^\ddagger$
Scenario 1: Clumped isotope temperatures are used to calculate mineral-water fractionation factors for all samples										
Upper aragonitic section										
1H-2-80 90C	0.8	0.8	3	13	-4.254	0.922	-0.023	0.007	-14.7	1.9
1H-2-80 25C	0.8	0.8	4	19	-3.152	1.062	-0.025	0.006	-14.0	1.9
2H-1-220 90C	2.2	2.1	2	8	-5.519	1.012	-0.027	0.008	-16.7	1.9
2H-1-320 90C	3.2	3.1	2	11	-6.151	1.029	-0.025	0.008	-16.9	2.0
2H-1-440 90C	4.4	4.4	3	16	-5.410	1.035	-0.017	0.012	-15.1	2.3
3H-1-550 90C	5.5	5.6	2	24	-2.898	1.077	-0.025	0.008	-13.7	2.0
3H-1-660 90C	6.6	7.2	2	24	-3.838	1.400	-0.026	0.009	-14.8	2.0
3H-2-715 90C	7.15	8.2	3	20	-7.056	1.067	-0.003	0.008	-14.8	2.1
3H-2-800 90C	8	10.1	4	22	-3.098	1.055	-0.026	0.010	-14.2	2.1
Lower calcitic / dolomitic section										
4H-2-A-1026 25C	10.26	16.0	1	19	-7.106	1.807	0.006	0.012	-13.5	2.9
5H-1-A-1120 25C	11.2	18.1	2	43	-4.048	1.021	-0.010	0.008	-12.9	2.0
5H-1-A-1245 25C	12.45	20.6	1	34	-5.608	1.482	-0.023	0.011	-16.1	2.3
5H-2-A-1300 25C	13	21.6	4	33	-5.709	1.125	0.003	0.014	-12.9	3.2
6H-1-A-1500 25C	15	24.6	1	29	-6.792	1.051	-0.008	0.011	-15.4	2.4
Scenario 2: Average clumped isotope temperature for Holocene samples (= 18 °C) is used to calculate mineral-water fractionation factors for lower calcitic / dolomitic samples										
Lower calcitic / dolomitic section										
4H-2-A-1026 25C	10.26	16.0	1	18	-7.363	0.825	0.007	0.010	-13.5	2.5
5H-1-A-1120 25C	11.2	18.1	2	18	-8.958	0.838	0.005	0.007	-15.3	2.3
5H-1-A-1245 25C	12.45	20.6	1	18	-8.781	0.798	-0.015	0.010	-18.3	2.2
5H-2-A-1300 25C	13	21.6	4	18	-8.688	0.871	0.013	0.013	-14.9	4.6
6H-1-A-1500 25C	15	24.6	1	18	-9.025	0.846	-0.001	0.010	-16.5	2.7
Scenario 3: A temperature of 5 °C lower than the average Holocene clumped isotope temperature (= 13 °C) is used to calculate mineral-water fractionation factors for the lower calcitic / dolomitic section										
Lower calcitic / dolomitic section										
4H-2-A-1026 25C	10.26	16.0	1	13	-8.383	0.834	0.010	0.011	-14.3	3.3
5H-1-A-1120 25C	11.2	18.1	2	13	-9.971	0.870	0.008	0.008	-16.1	2.6
5H-1-A-1245 25C	12.45	20.6	1	13	-9.808	0.833	-0.010	0.011	-18.6	2.4
5H-2-A-1300 25C	13	21.6	4	13	-9.787	0.815	0.016	0.014	-16.0	4.9
6H-1-A-1500 25C	15	24.6	1	13	-10.053	0.873	0.003	0.010	-17.1	2.9

§ All core samples IDs have the prefix "GLAD1-BL00-1E", which has been omitted for clarity

¶ These are the standard deviations of 500 Monte-Carlo computations accounting for uncertainty in carbonate isotopic composition (as reported in Table 3), formation temperature (as reported in Table 2, or = 1 °C for Scenarios 2 and 3), and mineral-water fractionation factors (± 0.00007 for $\alpha_{\text{mineral-water}}$ and ± 0.0008 for $^{18}\alpha_{\text{mineral-water}}$).

‡ These are the standard deviations of 500 Monte-Carlo computations including the uncertainties listed above, as well as uncertainty in the evaporation slope λ_{lake} (± 0.0005) and the $\Delta^{17}\text{O}$ of meteoric water ($\pm 0.005\text{‰}$).

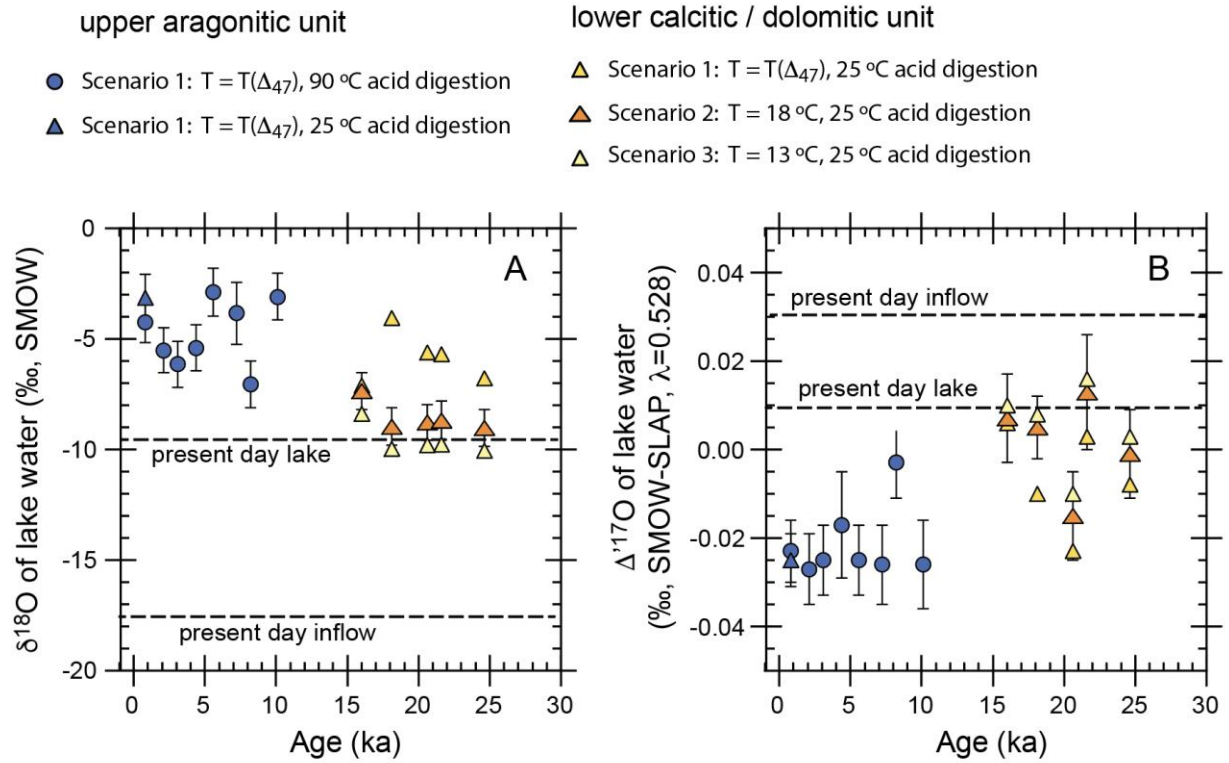


Figure 4. Calculated isotopic compositions of carbonate parent waters (= lake water). A) $\delta^{18}\text{O}$ values. B) $\Delta^{17}\text{O}$ values. Error bars are 1 standard deviation of the population of 500 Monte-Carlo calculations of isotopic composition for each sample. Error bars are omitted for clarity for Scenario 1 and Scenario 3 values.

evaporative efflux from the lake. The magnitude of this change is explored below in terms of implications for lake paleohydrology.

$\delta^{18}\text{O}$ of unevaporated precipitation

The reconstructed $\delta^{18}\text{O}$ of unevaporated catchment precipitation calculated using equations 9 and 10 is reported in Table 4 and shown in Figure 5. The average value for late glacial time was $-15.7 \pm 1.8\text{‰}$, while that for Holocene time was $-15.0 \pm 1.1\text{‰}$. These values overlap significantly and are not statistically distinct (unpaired t-test, $p = 0.38$). Therefore, we are unable to resolve any change in the $\delta^{18}\text{O}$ of precipitation in the Bear Lake catchment basin between late glacial and Holocene time, although the magnitude of change is a minimum estimate given the assumption of Holocene temperature. The $\delta^{18}\text{O}_{\text{rucp}}$ values are higher than $\delta^{18}\text{O}$ of river water presently entering the lake ($-17.6 \pm 1.4 \text{‰ } 1\sigma$; Passey and Ji, 2019 and unpublished data). However, in the modern calibration of Passey and Ji (2019), $\delta^{18}\text{O}_{\text{rucp}}$ values were consistently $\sim 2\text{‰}$ higher than $\delta^{18}\text{O}$ values of river waters entering the lakes, so we do not view the difference in late glacial + Holocene $\delta^{18}\text{O}_{\text{rucp}}$ and modern $\delta^{18}\text{O}$ of precipitation (as gauged by rivers entering Bear Lake) to be noteworthy. The influence of detrital carbonate acts to increase $\delta^{18}\text{O}$ and decrease $\Delta^{17}\text{O}$, which have opposing effects in terms of determining $\delta^{18}\text{O}_{\text{rucp}}$, so detrital carbonate is probably not responsible for the elevated $\delta^{18}\text{O}_{\text{rucp}}$ compared to modern river waters.

Paleohydrology of Bear Lake

Here we further investigate the paleohydrology of Bear Lake using a steady state isotopic mass balance model (Criss, 1999; see also Passey and Ji, 2019):

$$R_W = \frac{\alpha_{eq} \alpha_{diff} (1-h) R_I h X_E R_A}{X_E + \alpha_{eq} \alpha_{diff} (1-h) (1-X_E)} \quad \text{Equation 12}$$

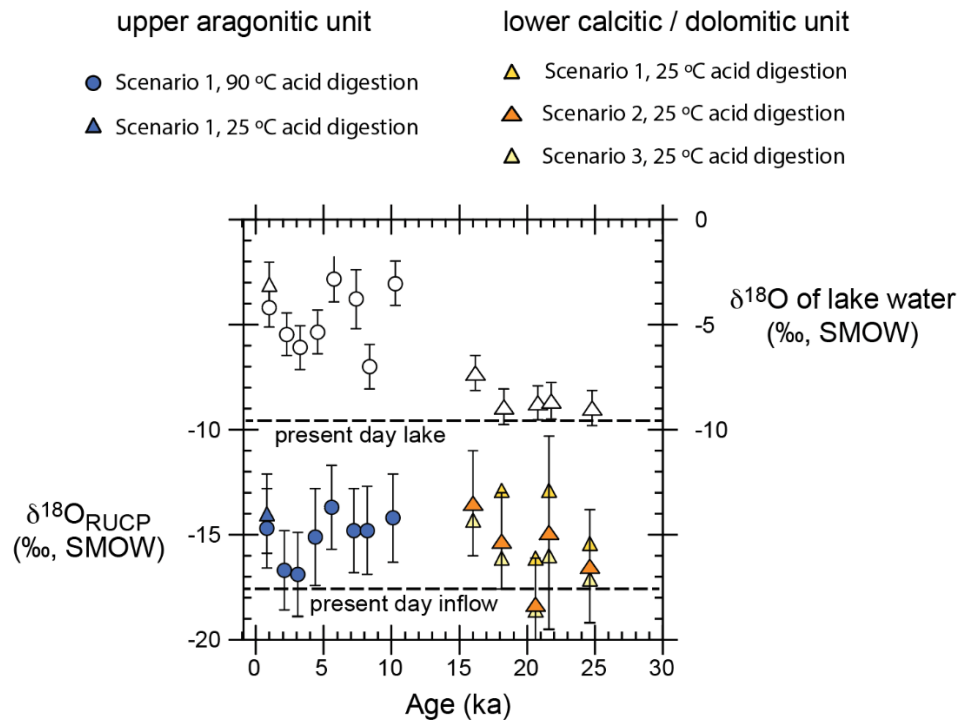


Figure 5. Reconstructed oxygen isotopic composition of unevaporated precipitation ($\delta^{18}\text{O}_{\text{RUCP}}$). Colored symbols show $\delta^{18}\text{O}_{\text{RUCP}}$, while open symbols show $\delta^{18}\text{O}$ of lake water for reference (Scenario 2 calculations). Error bars are 1 standard deviation of the population of 500 Monte-Carlo calculations of isotopic composition for each sample.

Where R_W , R_I , and R_A are the isotope ratios of lake water, inflow water + direct precipitation, and atmospheric water vapor, respectively, X_E is the fraction of outflux water lost to evaporation, h is relative humidity (normalized to the surface temperature of the lake), and α_{eq} and α_{diff} are the isotope fractionations associated with equilibrium between liquid water and water vapor (α_{eq}), and for water vapor transport from the lake to the free atmosphere (α_{diff}). In terms of $\Delta^{17}\text{O}$, only α_{eq} and R_I are well constrained, meaning that there are four relatively unconstrained parameters— h , X_E , R_A and α_{diff} . Therefore, it is not possible to solve for any single parameter. However, there may be portions of the parameter space that are ruled out by observed isotopic compositions. Figure 6 shows the predictions of Equation 11 in terms of $\Delta^{17}\text{O}$ plotted against h for several combinations of X_E , R_A and α_{diff} . In all cases, there is no combination of parameters with X_E values less than ~ 0.3 (i.e., less than 30% evaporative efflux) that can predict the observed isotopic composition of the lake during the late glacial or Holocene. We view the parameter ranges in Figure 6A and 6B to be the most probable, as the combination in Figure 6C does not accurately reflect the isotopic compositions of modern lakes in the western United States. Figure 6C is shown for reference because a value of $\alpha_{diff} = 1.014$ has been widely used by the isotope hydrology community, but in order to successfully predict the isotopic compositions of modern lakes, R_A values must be elevated (Figure 6B) rather than being in equilibrium with regional precipitation (Figure 6C).

Bear Lake was an endorheic lake (= closed basin, $X_E = 1$) prior to construction of the canals connecting Bear River to the lake, and the triple oxygen isotope data suggest that it was generally a closed basin lake during the Holocene. Given that X_E cannot be greater than 1, there is no combination of parameters where relative humidity can be greater than $\sim 60\%$ (Figures 6A and 6B), suggesting that relative humidity during the Holocene was similar to present (mean annual $h = 55\%$), or that h was lower and X_E was slightly less than 1 (for example, owing to seepage out of the lake basin or periodic overflow across the threshold into Bear River).

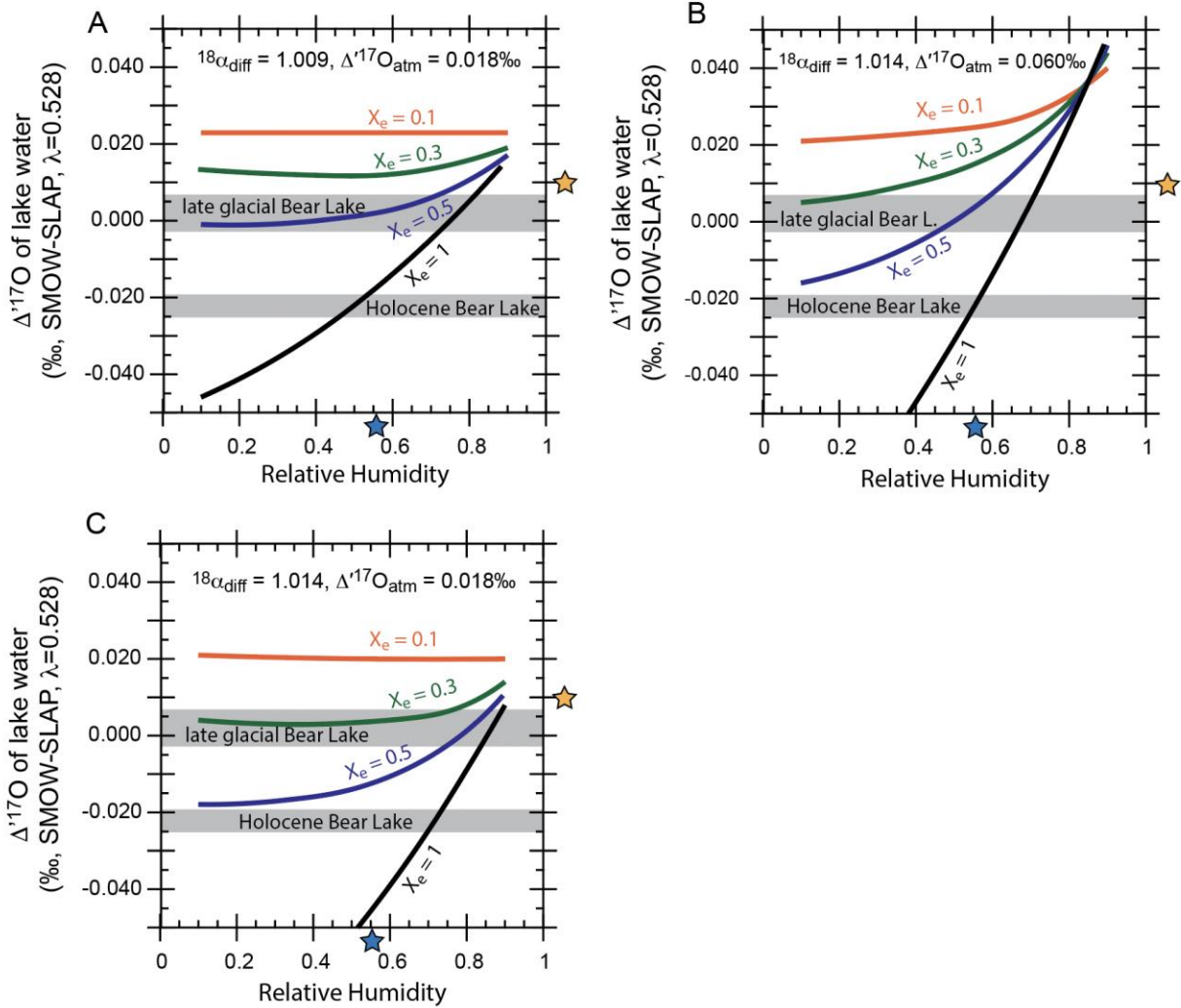


Figure 6. $\Delta^{17}\text{O}$ of reconstructed lake water in the context of $\Delta^{17}\text{O}$ versus relative humidity predicted from steady-state isotopic mass balance modeling. In each figure, the gray bands show the 1 SEM range of the reconstructed $\Delta^{17}\text{O}$ of lake water. Orange stars show the present-day $\Delta^{17}\text{O}$ of the lake, and the blue stars show the present-day mean annual relative humidity. A) Our preferred scenario where $^{18}\alpha_{\text{diff}} = 1.009$ and $\Delta^{17}\text{O}_{\text{atm}} = 0.018\text{‰}$. B) Another plausible scenario where $^{18}\alpha_{\text{diff}} = 1.014$ and $\Delta^{17}\text{O}_{\text{atm}} = 0.060\text{‰}$. We view both parameter combinations as being plausible because they successfully predict the compositions of modern western U. S. lakes (Passey and Ji, 2019). C) A scenario using $^{18}\alpha_{\text{diff}} = 1.014$ and $\Delta^{17}\text{O}_{\text{atm}} = 0.018\text{‰}$. Although these values have been widely used in lake balance modeling in δD – $\delta^{18}\text{O}$ space, however it does not successfully predict modern observations of lake triple oxygen isotope compositions.

During late glacial times, the triple oxygen isotope data suggest that >40% of water exited the lake via evaporation (Figures 6A and 6B). The inferred value of X_E scales with relative humidity, with higher relative humidity requiring higher X_E (and vice versa) to account for the observed isotopic composition of the lake. Although the presence of pluvial lakes during this time interval attests to higher precipitation to evaporation (P/E) ratios in the western U. S. during this time, this does not necessarily mean that relative humidity was substantially higher. LGM climate simulations presented by Bush and Philander (1999) show that zonally averaged relative humidity was within a few percent of modern except in the immediate vicinity of the ice sheets in North America and elsewhere. If we assume that relative humidity was within 10% of the modern value, then X_E must have been ~ 40% or higher for the late glacial Bear Lake.

Comparison to other records of precipitation $\delta^{18}\text{O}$ change in the western U. S.

Figure 7 shows the $\delta^{18}\text{O}_{\text{rncp}}$ values for Bear Lake plotted along with records of $\delta^{18}\text{O}$ change from the Leviathan + Pinnacle cave speleothem record from eastern Nevada (Lachniet et al. 2014, 2017) and the Devil's Hole record from southeast Nevada. For Devil's Hole, $\delta^{18}\text{O}_{\text{water}}$ was calculated using newly published clumped isotope data suggesting that temperatures in Devil's Hole remained relatively constant at 33.7 ± 1 °C over the entire time interval of interest (Bajnai et al., 2021). For the Leviathan and Pinnacle records, we used the present-day cave temperatures. If late glacial temperatures were (for example) 5 °C lower, then $\delta^{18}\text{O}_{\text{water}}$ values would be ~1‰ lower than shown in Figure 7 (this applies for both the Bear Lake and Pinnacle Cave records). Uncertainties in temperature notwithstanding, these records show that $\delta^{18}\text{O}$ of precipitation changed by no more than +2 – 3‰ from the late glacial to the Holocene. The Leviathan + Pinnacle record shows the most change, but some of this may have been due to a change in seasonality of precipitation or changes in evaporation (Huth et al., 2022). The three archives are fundamentally very different, with Devil's Hole representing a regionally integrated

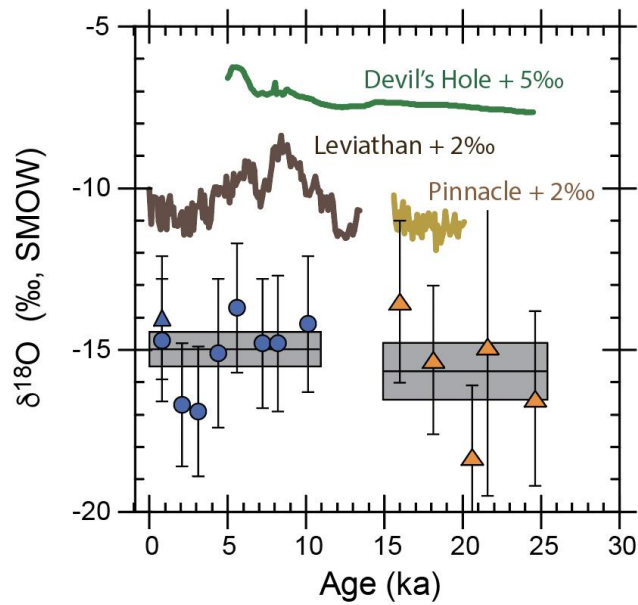


Figure 7. Comparison of $\delta^{18}\text{O}$ of reconstructed unevaporated precipitation to other records. The blue circles and orange triangles show $\delta^{18}\text{O}_{\text{RUCP}}$ for the upper aragonitic unit and lower calcitic / dolomitic unit at Bear Lake calculated for Scenario 2. Error bars are 1 standard deviation of the population of 500 Monte-Carlo calculations of isotopic composition for each sample. For the Leviathan Cave and Pinnacle Cave records (Lachniet et al., 2014; 2017), $\delta^{18}\text{O}$ of cave drip water was calculated assuming $T =$ modern cave temperature. 2‰ was then added to these values to facilitate viewing. For Devil's Hole (Moseley et al., 2016), $\delta^{18}\text{O}$ of groundwater was calculated using $T(\Delta_{47})$ from Bajnai et al., (2021) ($= 33.4$ °C), and 5‰ was added to facilitate viewing.

groundwater system, Leviathan + Pinnacle montane cave environments, and Bear Lake an intermontane lake basin. Despite these differences, the records are similar in their indication that 1) glacial $\delta^{18}\text{O}$ was lower than Holocene $\delta^{18}\text{O}$, but that 2) the magnitude of $\delta^{18}\text{O}$ change was relatively small.

Our results can be added to the set of proxy data used to assess the accuracy of Earth System Models. Figure 8 shows the LGM-late Holocene $\delta^{18}\text{O}_{\text{precipitation}}$ difference ($\Delta\delta^{18}\text{O}_p$) modeled using iCESM (isotope-enabled Community Earth System Model) by Tierney et al. (2020). The -0.7‰ $\Delta\delta^{18}\text{O}_p$ value for Bear Lake catchment precipitation (diamond symbol in Figure 8) supports the model's prediction that this region experienced only small changes in $\delta^{18}\text{O}_{\text{precipitation}}$. The iCESM predictions of $\Delta\delta^{18}\text{O}_p$ for this region transition from slightly positive in the westernmost U. S. to slightly negative towards the east. Because of the influence of detrital carbonate, and the assumption of Holocene temperature for late glacial carbonates, the actual value for $\Delta\delta^{18}\text{O}_p$ at Bear Lake is -0.7‰ or lower (more negative).

CONCLUSIONS

The application of clumped isotopes, triple oxygen isotopes, and stepped-temperature acid digestions has revealed new information about the stable isotope record from Bear Lake. Some of the more salient findings include:

- Detrital carbonate significantly affects the isotopic signal from the lower portion of the record. The effect of detrital carbonate is to mute the degree of change from the late glacial to the Holocene both in $\delta^{13}\text{C}$ and $\delta^{18}\text{O}$. Use of 25 °C acid digestions reduces the influence of the detrital component on measured isotopic compositions. Taking this into account, the magnitudes of change in $\delta^{13}\text{C}$ and $\delta^{18}\text{O}$ of authigenic carbonate were at least $+5.6\text{‰}$ and $+4.8\text{‰}$, respectively.
- Making reasonable assumptions about authigenic carbonate growth temperatures, Bear Lake water increased in $\delta^{18}\text{O}$ by at least 4‰ from the late glacial to the Holocene. This change was

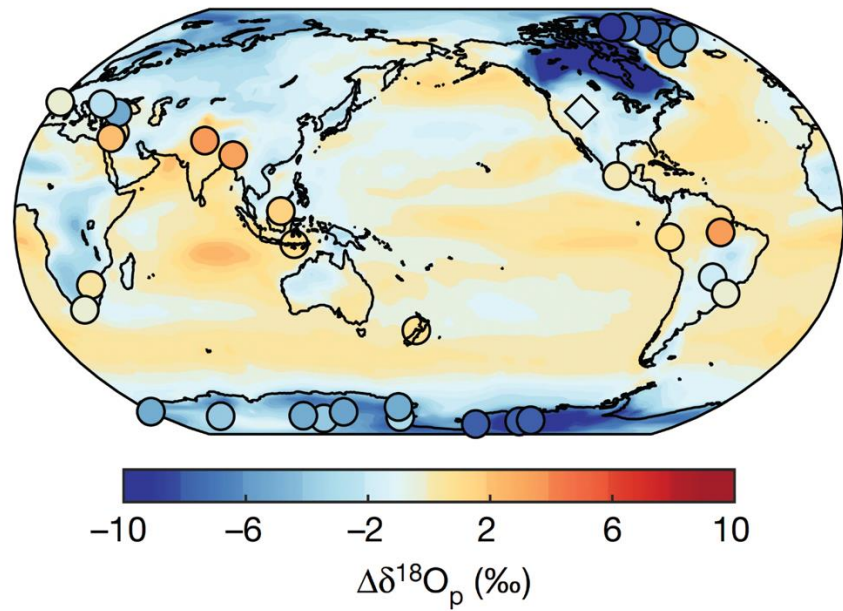


Figure 8. Changes from the LGM to late Holocene in the $\delta^{18}\text{O}$ of precipitation ($\Delta\delta^{18}\text{O}_p$). The background field shows modeled $\Delta\delta^{18}\text{O}_p$ from iCESM simulations presented by Tierney et al. (2020). The symbols show proxy-reconstructed $\Delta\delta^{18}\text{O}_p$. Circles are from ice core and speleothem data. The diamond shows the minimum $\Delta\delta^{18}\text{O}_p$ reconstructed for Bear Lake (-0.7‰ or more negative). Figure modified from Tierney et al., (2020).

accompanied by a 0.02 ‰ decrease in $\Delta^{17}\text{O}$, and the triple oxygen isotope slope linking the pooled late glacial to pooled Holocene data is 0.522. This indicates that increased evaporation during the Holocene compared to the late glacial was the major driver of the change in lake water $\delta^{18}\text{O}$.

- The reconstructed $\Delta^{17}\text{O}$ values of lake water, interpreted in the context of a steady-state isotope mass balance model, indicate that Bear Lake had a significant evaporative efflux during late glacial time (>40% of total water loss via evaporation). During the Holocene, Bear Lake was most likely a closed-basin lake, just as the lake was in historical times prior to diversion of Bear River water into the lake.
- The reconstructed $\delta^{18}\text{O}$ of unevaporated precipitation was slightly lower (-0.7‰) during late glacial times and Holocene times. The difference is not statistically significant, but the late glacial estimate of $\delta^{18}\text{O}$ is an upper limit due to the influence of detrital carbonate and assumptions about authigenic carbonate mineralization temperatures. The modest difference between late glacial and Holocene time is consistent with the predictions for the western U. S. from iCESM, supporting the validity of that model.

In addition to these findings, part of the motivation of this study was to assess the use of triple oxygen isotopes and clumped isotopes in lake carbonate-based paleoclimate / paleohydrology reconstruction. These methods brought a significant amount of new information to light, despite the challenges related to detrital carbonate contamination. In lake sediments lacking significant detrital carbonate, accurate temperature reconstruction should be possible using clumped isotopes, and the determination of lake water isotopic compositions, and $\delta^{18}\text{O}$ of unevaporated catchment precipitation, would be considerably more straightforward. The combination of triple oxygen and clumped isotopes for the first time allows for reconstruction of changes in the $\delta^{18}\text{O}$ of precipitation using lake archives.

Among other outcomes, model-proxy comparisons (e.g., Figure 8) could be extended beyond ice-core and

speleothem records to include the lacustrine records, which would greatly improve the spatial resolution of such comparisons.

In terms of the Bear Lake record, much work remains to be done. We have shown that acid digestion at 25 °C yields superior results compared to higher temperature reactions, and an obvious next step would be to generate a higher-resolution record of the late glacial to present portion of the core, and with more replicate analyses. Opportunities exist for additional semiquantitative XRD work (e.g., analyzing unknowns in the context of synthetic reference sediments with known fractions of dolomite, calcite, aragonite), including XRD work on residual sediment following stepped acid digestion. Such results could inform mass balance models for estimating the fractional contribution of detrital carbonate to measured isotopic compositions. Finally, the BL00-1E core extends back to ca. 250 ka, meaning that 90% of the time contained in the record remains unexplored with respect to triple oxygen and clumped isotopes. This would permit comparative paleohydrology across multiple interglacial and glacial intervals and provide new insights into the long term hydrologic and climatic evolution of the Bear Lake catchment basin.

ACKNOWLEDGEMENTS

I would like to thank my undergraduate advisor Jenn Cotton for introducing me to the exciting world of isotope geochemistry. Without her support I would not have decided to go to graduate school and would not be writing this thesis. To her I am grateful beyond words. I would also like to thank my graduate advisor Ben Passey who gifted me many laboratory and writing skills one builds upon over time through the act of doing. I gained a great deal of confidence troubleshooting and working on the inner parts of our mass spectrometers throughout my time in graduate school and the skills I attained while working in the Isopaleo lab are ones that I am truly grateful for. Lastly I appreciate the support of all my friends, family, and pets (near and far) who remind me just how much love is a necessity to live well.

REFERENCES

- Angert, A., Cappa, C.D., & DePaolo, D.J.**, 2004. Kinetic ^{17}O effects in the hydrologic cycle: Indirect evidence and implications. *Geochimica et Cosmochimica Acta* **68**(17), 3487–3495.
- Baker, L., Franchi, I. A., Maynard, J., Wright, I. P., & Pillinger, C. T.**, 2002. A Technique for the Determination of $^{18}\text{O}/^{16}\text{O}$ and $^{17}\text{O}/^{16}\text{O}$ Isotopic Ratios in Water from Small Liquid and Solid Samples. *Analytical Chemistry* **74**(7), 1665–1673.
- Bajnai, D., Coplen, T.B., Methner, K., Löffler, N., Krsnik, E., Fiebig, J.**, 2021. Devils hole calcite was precipitated at $\pm 1^\circ\text{C}$ stable aquifer temperatures during the last half million years. *Geophysical Research Letters* **48**, e2021GL093257.
- Barkan, E., & Luz, B.**, 2005. High precision measurements of $^{17}\text{O}/^{16}\text{O}$ and $^{18}\text{O}/^{16}\text{O}$ ratios in H_2O . *Rapid Communications in Mass Spectrometry* **19**(24), 3737–3742.
- Barkan, E., & Luz, B.**, 2007. Diffusivity fractionations of $\text{H}_2^{16}\text{O}/\text{H}_2^{17}\text{O}$ and $\text{H}_2^{16}\text{O}/\text{H}_2^{18}\text{O}$ in air and their implications for isotope hydrology. *Rapid Communications in Mass Spectrometry* **21**, 2999–3005.
- Barkan, E., Musan, I., Luz, B.**, 2015. High-precision measurements of $\delta^{17}\text{O}$ and ^{17}O -excess of NBS–19 and NBS–18. *Rapid Communications in Mass Spectrometry* **29**, 2219–2224.
- Barnett, T. P., Pierce, D. W., Hidalgo, H. G., Bonfils, C., Santer, B. D., Das, T., et al.**, 2008. Human-Induced Changes in the Hydrology of the Western United States. *Science* **319**(5866), 1080–1083.
- Bergmann, K.D., Al Balushi, S.A.K., Mackey, T.J., Grotzinger, J.P., Eiler, J.M.**, 2018. A 600-million-year carbonate clumped-isotope record from the Sultanate of Oman. *Journal of Sedimentary Research* **88**(8), 960–979.
- Bernasconi, S. and 60 others**, 2021. InterCarb: A Community Effort to Improve Interlaboratory Standardization of the Carbonate Clumped Isotope Thermometer Using Carbonate standards. *Geochemistry, Geophysics, Geosystems* **22**, e2020GC009588.

- Bright, J., Kaufman, D. S., Forester, R. M., & Dean, W. E.,** 2006. A continuous 250,000yr record of oxygen and carbon isotopes in ostracods and bulk-sediment carbonate from Bear Lake, Utah-Idaho. *Quaternary Science Reviews* **25**(17), 2258–2270.
- Broecker, W.,** 2010. Long-Term Water Prospects in the Western United States. *Journal of Climate* **23**(24), 6669–6683.
- Bush, A. B. G., Philander, S. G. H.,** 1999. The climate of the Last Glacial Maximum: Results from a coupled ocean-atmosphere general circulation model. *Journal of Geophysical Research* **104**, 24509-24525.
- Colman, S. M., Rosenbaum, J. G., Kaufman, D. S., Dean, W. E., & McGeehin, J. P.,** 2009. Radiocarbon ages and age models for the past 30,000 years in Bear Lake, Utah and Idaho. In J. G. Rosenbaum & D. S. Kaufman, *Paleoenvironments of Bear Lake, Utah and Idaho, and its catchment: Geological Society of America Special Paper 450*, 133–144.
- Craig, H.,** 1961. Isotopic Variations in Meteoric Waters. *Science* **133**(3465), 1702–1703.
- Criss, R. E.,** 1999. Principles of Stable Isotope Distribution. *Oxford University Press* New York.
- Dansgaard, W.,** (1964). Stable isotopes in precipitation. *Tellus* **16**(4), 436–468.
- Dean, W., Rosenbaum, J., Skipp, G., Colman, S., Forester, R., Liu, A., et al.,** 2006. Unusual Holocene and late Pleistocene carbonate sedimentation in Bear Lake, Utah and Idaho, USA. *Sedimentary Geology* **185**(1), 93–112.
- Dean, W. E.,** 2009. Endogenic carbonate sedimentation in Bear Lake, Utah and Idaho, over the last two glacial- interglacial cycles. In J. G. Rosenbaum & D. S. Kaufman, *Paleoenvironments of Bear Lake, Utah and Idaho, and its catchment: Geological Society of America Special Paper 450*, 169-196

- Degens, E.T., Epstein, S.,** 1964. Carbon and oxygen isotope ratios in coexisting calcites and dolomites from recent and ancient sediments. *Geochimica et Cosmochimica Acta* **28**, 23-44.
- Dennis, K. J., Affek, H. P., Passey, B. H., Schrag, D. P., & Eiler, J. M.,** 2011. Defining an absolute reference frame for ‘clumped’ isotope studies of CO₂. *Geochimica et Cosmochimica Acta* **75**(22), 7117–7131.
- Defliese, W.F., Hren, M.T., Lohmann, K.C.,** 2015. Compositional and temperature effects of phosphoric acid fractionation on Δ_{47} analysis and implications for discrepant calibrations. *Chemical Geology* **396**, 51-60.
- Dinçer, T.,** 1968. The use of oxygen 18 and deuterium concentrations in the water balance of lakes. *Water Resources Research* **4**, 1289–1306.
- Ferry, J.M., Passey, B.H., Vasconcelos, C., Eiler, J.M.,** 2011. Formation of dolomite at 40–60 °C in the Latemar carbonate buildup, Dolomites, Italy, from clumped isotope thermometry. *Geology* **39**, 571-574.
- Friedrich, K., Grossman, R. L., Huntington, J., Blanken, P. D., Lenters, J., Holman, K. D., et al.,** 2017. Reservoir Evaporation in the Western United States: Current Science, Challenges, and Future Needs. *Bulletin of the American Meteorological Society* **99**(1), 167–187.
- Gat, J. R.,** 1996. Oxygen and Hydrogen Isotopes in the Hydrologic Cycle. *Annual Review of Earth and Planetary Sciences* **24**(1), 225–262.
- Gat, Joel R., Bowser, C. J., & Kendall, C.,** 1994. The contribution of evaporation from the Great Lakes to the continental atmosphere: estimate based on stable isotope data. *Geophysical Research Letters* **21**(7), 557–560.
- Gázquez, F., Morellón, M., Bauska, T., Herwartz, D., Surma, J., Moreno, A., et al.,** 2018. Triple oxygen and hydrogen isotopes of gypsum hydration water for quantitative paleo-humidity reconstruction. *Earth and Planetary Sciences Letters* **481**, 177–188.

- Gibson, J. J., Birks, S. J., Yi, Y.,** 2015. Stable isotope mass balance of lakes: a contemporary perspective. *Quaternary Science Reviews* **131 part B**, 316–328.
- Ghosh, P., Adkins, J., Affek, H., Balta, B., Guo, W., Schauble, E.A., Schrag, D., Eiler, J.M.,** 2006. ^{13}C – ^{18}O bonds in carbonate minerals: A new kind of paleothermometer. *Geochimica et Cosmochimica Acta* **70**, 1439-1456.
- Hren, M.T., Sheldon, N.D.,** 2012. Temporal variations in lake water temperature: Paleoenvironmental implications of lake carbonate $\delta^{18}\text{O}$ and temperature records. *Earth and Planetary Science Letters* **337-338**, 77-84.
- Huth, T.E., Passey, B.H., Cole, J.E., Lachniet, M.S., McGee, D., Denniston, R.F., Truebe, S., Levin, N.E.,** 2022. A framework for triple oxygen isotopes in speleothem paleoclimatology. *Geochimica et Cosmochimica Acta* **319**, 191-219.
- Huntington, K.W., Wernicke, B.P., Eiler, J.M.,** 2010. Influence of climate change and uplift on Colorado Plateau paleotemperatures from carbonate clumped isotope thermometry. *Tectonics* **29(3)** TC3005.
- Kaufman, D. S., Bright, J., Dean, W. E., Rosenbaum, J. G., Moser, K., Anderson, R. S., et al.,** 2009. A quarter-million years of paleoenvironmental change at Bear Lake, Utah and Idaho. In J. G. Rosenbaum & D. S. Kaufman, *Paleoenvironments of Bear Lake, Utah and Idaho, and its catchment: Geological Society of America Special Paper 450*, 311-351.
- Kelson, J.R., Petersen, S.V., Niemi, N.A., Passey, B.H., Curley, A.N.,** 2022. Looking upstream with clumped and triple oxygen isotopes of estuarine oyster shells in the early Eocene of California, USA. *Geology*.
- Kim, S.-T., & O'Neil, J. R.,** 1997. Equilibrium and nonequilibrium oxygen isotope effects in synthetic carbonates. *Geochimica et Cosmochimica Acta* **61(16)**, 3461–3475.

- Kim, S.-T., O'Neil, J. R., Hillaire-Marcel, C., & Mucci, A.,** 2007a. Oxygen isotope fractionation between synthetic aragonite and water: Influence of temperature and Mg²⁺ concentration. *Geochimica et Cosmochimica Acta* **71**(19), 4704–4715.
- Kim, S.-T., Mucci, A., & Taylor, B. E.,** 2007b. Phosphoric acid fractionation factors for calcite and aragonite between 25 and 75 °C: Revisited. *Chemical Geology* **246**(3–4), 135–146.
- Lachniet, M., Denniston, R. F., Asmerom, Y., Polyak, V. J.,** 2014. Orbital control of western North America atmospheric circulation and climate over two glacial cycles. *Nature Communications* **5**, 3805.
- Lachniet, M., Asmerom, Y., Polyak, V., & Denniston, R.,** 2017. Arctic cryosphere and Milankovitch forcing of Great Basin paleoclimate. *Scientific Reports* **7**(1), 12955.
- Leng, M. J., & Marshall, J. D.,** 2004. Palaeoclimate interpretation of stable isotope data from lake sediment archives. *Quaternary Science Reviews* **23**(7), 811–831.
- Li, H., Liu, X., Arnold, A., Elliott, B., Flores, R., Kelley, A.M., Tripathi, A.,** 2021. Mass 47 clumped isotope signatures in modern lacustrine authigenic carbonates in Western China and other regions and implications for paleotemperature and paleoelevation reconstructions. *Earth and Planetary Science Letters* **562**, 116840.
- Liu, X., Deng, W., Wei, G.,** 2019. Carbon and oxygen isotopic analyses of calcite in calcite-dolomite mixtures: Optimization of selective acid extraction. *Rapid Communications in Mass Spectrometry* **33**, 411–418.
- Moseley, G. E., Edwards, R. L., Wendt, K. A., Cheng, H., Dublyansky, Y., Lu, Y., et al.,** 2016. Reconciliation of the Devils Hole climate record with orbital forcing. *Science* **351**(6269), 165–168.

- Osman M.B., Tierney, J.E., Zhu, J., Tardif, R., Hakim, G.J., King, J., Poulsen, C.J.,** 2021. Globally resolved surface temperatures since the Last Glacial Maximum. *Nature* **599**, 239–244.
- Passey, B.H., Levin, N.E., Cerling, T.E., Brown, F.H., Eiler, J.M.,** 2010. High-temperature environments of human evolution in East Africa based on bond ordering in paleosol carbonates. *Proceedings of the National Academy of Sciences, USA* **107**, 11245-11249.
- Passey, B. H., & Ji, H.,** 2019. Triple oxygen isotope signatures of evaporation in lake waters and carbonates: A case study from the western United States. *Earth and Planetary Science Letters*, **518**, 1–12.
- Passey, B. H., Hu, H., Ji, H., Montanari, S., Li, S., Henkes, G. A., & Levin, N. E.,** 2014. Triple oxygen isotopes in biogenic and sedimentary carbonates. *Geochimica et Cosmochimica Acta* **141**, 1–25.
- Petersen, S.V., and 29 others,** 2019. Effects of improved ^{17}O correction on interlaboratory agreement in clumped isotope calibrations, estimates of mineral-specific offsets, and temperature dependence of acid digestion fractionation. *Geochemistry, Geophysics, Geosystems* **20**, 3495-3519.
- Rosenbaum, J. G., & Heil, C. W.,** 2009. The glacial/deglacial history of sedimentation in Bear Lake, Utah and Idaho. In J. G. Rosenbaum & D. S. Kaufman, *Paleoenvironments of Bear Lake, Utah and Idaho, and its catchment: Geological Society of America Special Paper 450*, 247-261.
- Ryb, U., Lloyd, M.K., Eiler, J.M.,** 2021. Carbonate clumped isotope constraints on burial, uplift and exhumation histories of the Colorado Plateau. *Earth and Planetary Science Letters* **566**, 116964.
- Schauble, E.A., Ghosh, P., Eiler, J.M.,** 2006. Preferential formation of ^{13}C – ^{18}O bonds in carbonate minerals, estimated using first-principles lattice dynamics. *Geochimica et Cosmochimica Acta* **70**, 2510-2529.
- Schoenemann, S. W., Schauer, A. J., & Steig, E. J.,** 2013. Measurement of SLAP2 and GISP $\delta^{17}\text{O}$ and proposed VSMOW-SLAP normalization for $\delta^{17}\text{O}$ and ^{17}O excess. *Rapid Communications in Mass Spectrometry* **27**(5), 582– 590.

- Seltzer, A.M., Ng, J., Aeschbach, W., Kipfer, R., Kulongoski, J.T., Severinghaus, J.P., Stute, M.,** 2021. Widespread six degrees Celsius cooling on land during the Last Glacial Maximum. *Nature* **593**, 228–232.
- Shenton, B.J., Grossman, E.L., Passey, B.H., Henkes, G.A., Becker, T.P., Laya, J.C., Perez-Huerta, A., Becker, S.P., Lawson, M.,** 2015. Clumped isotope thermometry in deeply buried sedimentary carbonates: The effects of bond reordering and recrystallization. *Geological Society of America Bulletin* **127**, 1036-1051.
- Surma, J., Assonov, S., Bolourchi, M. J., & Staubwasser, M.,** 2015. Triple oxygen isotope signatures in evaporated water bodies from the Sistan Oasis, Iran. *Geophysical Research Letters* **42**(20), 8456–8462.
- Surma, Jakub, Assonov, S., Herwartz, D., Voigt, C., & Staubwasser, M.,** 2018. The evolution of ¹⁷O-excess in surface water of the arid environment during recharge and evaporation. *Scientific Reports* **8**.
- Tierney, J. E., Zhu, J., King, J., Malevich, S. B., Hakim, G. J., Poulsen, C. J.,** 2020. Glacial cooling and climate sensitivity revisited. *Nature* **584**, 569-573.
- Urey, H. C.,** 1948. Oxygen Isotopes in Nature and in the Laboratory. *Science* **108**(2810), 489–496.
- Wang, Z., Schauble, E.A., Eiler, J.M.,** 2004. Equilibrium thermodynamics of multiply substituted isotopologues of molecular gases. *Geochimica et Cosmochimica Acta* **68**, 4779-4797.
- Wostbrock, J.A.G., Cano, E.J., Sharp, Z.D.,** 2020. An internally consistent triple oxygen isotope calibration of standards for silicates, carbonates and air relative to VSMOW2 and SLAP2. *Chemical Geology* **533**, 11

